Assessing the utility of barium isotopes to trace Eurasian riverine freshwater inputs to the Arctic Ocean

Luke Bridgestock[1]*, Joseph Nathan[1], Yu-Te Hsieh[1], Phil Holdship[1], Don Porcelli[1], Per S. Andersson[2] and Gideon M. Henderson[1]

[1]Department of Earth Science, University of Oxford, South Parks Road, Oxford, OX1 3AN, UK

[2]Laboratory for Isotope Geology, Swedish Museum of Natural History, Stockholm Sweden

*Corresponding author; ljb212@cam.ac.uk

Present address (Luke Bridgestock): Department of Earth Sciences, University of Cambridge, Downing Street, Cambridge, CB2 3EQ, UK

Abstract

Tracing riverine freshwater transport pathways within the Arctic Ocean is key to understanding changes in Arctic Ocean freshwater inventories. Dissolved Ba concentrations have been used in this capacity but are compromised by non-conservative processes. To assess the potential for Ba isotopes to provide insights into the impact of such processes on Arctic Ocean dissolved Ba inventories, Ba concentration and isotope data for surface seawater samples from the Siberian Shelf and Bering Sea/Strait are presented. These samples capture the mixing of riverine freshwater discharged by the rivers Yenisey, Lena and Ob, with Atlantic and Pacific derived seawater, which are traced by relationships between salinity, Ba concentration and $\delta^{138/134}$Ba. The $\delta^{138/134}$Ba of net river inputs, following modification by estuarine processes, are constrained to be 0.31 ± 0.04 ‰, 0.20 ± 0.06 ‰ and 0.23 ± 0.04 ‰, for the rivers Yenisey, Lena and Ob respectively. These values are used to estimate an average $\delta^{138/134}$Ba for Eurasian river freshwater input to the Arctic Ocean of 0.23 ± 0.04 ‰. The Ba concentration and $\delta^{138/134}$Ba of Lena River freshwater transported across the Laptev Sea are modified by non-conservative processes. These non-conservative processes do not result in distinctive modification of dissolved Ba concentration-$\delta^{138/134}$Ba mixing relationships between Eurasian riverine freshwater and Arctic seawater, which unfortunately limits the potential of Ba isotopes to improve tracing riverine freshwater sources in the central Arctic Ocean basins using dissolved Ba inventories. More generally the results of this study help advance understanding of Ba isotope cycling in the environment and their development as an emerging tracer of marine processes.

1. Introduction

The surface of the Arctic Ocean contains a large amount of freshwater, which stratifies the water column controlling circulation, sea-ice formation, and biological productivity (Carmack et al., 2016). The export of freshwater stored in the Arctic Ocean to the North Atlantic can also influence global meridional overturning circulation (Aagaard and Carmack, 1989). The storage, distribution and export of Arctic Ocean freshwater have varied over the past century, with particularly pronounced changes during recent decades, which have important implications for both regional and global climate (Rabe et al., 2014, Proshutinski et al., 2015, Haine et al., 2015, Alkire et al., 2017). River inputs are the main source of Arctic Ocean freshwater, contributing 4200 ± 420 km^3 yr^{-1}, along with net precipitation (2200 ± 220 km^3 yr^{-1}) and the inflow of low salinity Pacific seawater through the Bering Strait (2640 ± 100 km^3 yr^{-1}) (Haine et al., 2015). Freshwater distribution within the Arctic Ocean is further controlled by the seasonal formation and melting of sea-ice (e.g. Rosén et al., 2015), and changes in wind driven circulation (Proshutinski and Johnson, 1997, Steele and Boyd, 1998, Johnson and Polyakov, 2001, Morison et al., 2012).

Unraveling the roles of the multitude of freshwater sources that govern Arctic Ocean freshwater distributions requires the use of multiple geochemical tracers. Oxygen isotopes and nutrients (phosphate and nitrate) are routinely used to quantify ice melt/formation, Pacific inflow and meteoric (river discharge and net precipitation) contributions to Arctic Ocean freshwater inventories (e.g. Yamamoto-Kawai et al., 2008, Rosén et al., 2015). Dissolved Ba concentrations have further been used to distinguish between freshwater inputs from Eurasian versus North American rivers (Guay and Falkner, 1997, Macdonald et al., 1999, Guay et al., 2001, Taylor et al.,

2003, Dodd et al., 2009, Guay et al., 2009, Yamamoto-Kawai et al., 2010, Roeske et al., 2012, Charette et al., 2020). The use of this tracer has helped to reveal the role of riverine freshwater transport pathways for controlling key features of Arctic Ocean hydrography. Notably, that Eurasian riverine freshwater is an important component of the large freshwater inventory stored in the Beaufort Gyre (Guay et al., 2009), and of freshwater exported to the North Atlantic via the Fram Strait (Taylor et al., 2003, Dodd et al., 2009). By contrast, this tracer suggests freshwater inputs from the major North American river, the Mackenzie, do not make significant contributions to freshwater inventories in the central Arctic basins, and are instead are predominantly exported via the Canadian Arctic Archipelago (Guay et al., 2009).

The utility of dissolved Ba to trace Arctic Ocean riverine freshwater relies upon a difference in Ba concentration between freshwater inputs from major Eurasian and North American rivers (Guay and Falkner, 1998). This approach assumes that the Ba concentrations of these freshwater inputs are constant and that Ba behaves conservatively within the Arctic Ocean. Both of these assumptions, however, are questionable. In particular, dissolved Ba does not behave conservatively in the ocean, being removed from the upper water column and regenerated at depth in response to the production and export of organic matter (e.g. Jacquet et al., 2016). Non-conservative depletions and enrichments of dissolved Ba have been documented in the Barents Sea, Laptev Sea, Chukchi Sea, Gulf of Amundsen and to the north of Svalbard (Guy and Falkner, 1997, Abrahamsen et al., 2009, Thomas et al., 2011, Roeske et al., 2012, Hendry et al., 2018), regions that represent important transport pathways of major riverine freshwater and seawater sources to/from the central Arctic Ocean basins. Barium inputs from continental margins, via submarine groundwater discharge and/or diagenetic release from sediments (e.g. Mayfield et al., 2021) could

further impact the use of dissolve Ba as a conservative tracer of Arctic Ocean freshwater sources. Both biological productivity and trace metal inputs from Arctic margins have increased in recent decades in response to declining sea-ice cover and permafrost thawing (Arrigo and van Dijken, 2015, Williams and Carmack, 2015, Kipp et al., 2018). With these on-going changes the utility of dissolved Ba to trace riverine freshwater transport within the Arctic Ocean will become increasingly questionable without additional constraints (Abrahamsen et al., 2009).

Stable barium isotope variations are a new tool that can provide additional insights into marine Ba sources and the processes controlling marine Ba cycling. The cycling of Ba between the surface and deep ocean, linked to the biological carbon pump, is associated with significant Ba isotope fractionation resulting in coupled changes in dissolved Ba concentration and isotope composition (Horner et al., 2015, Bates et al., 2017, Hsieh and Henderson, 2017, Bridgestock et al., 2018, Geyman et al., 2019, Cao et al., 2020a, Cao et al., 2020b). Riverine and submarine groundwater discharge inputs could potentially result in mixing relationships between dissolved Ba concentrations and isotope compositions that are distinct from those resulting from these non-conservative marine processes (Hsieh and Henderson, 2017, Mayfield et al., 2021, Bridgestock et al., 2021). These systematics could be exploited to resolve the impact of biogeochemical cycling versus conservative mixing on Arctic Ocean dissolved Ba distributions. In turn this would improve the application of Ba to reliably trace riverine freshwater transport pathways within central Arctic Ocean basins. The utility of such an approach depends on the specific Ba concentration-isotope composition relationships produced by riverine freshwater-seawater mixing and non-conservative Ba cycling in the Arctic Ocean. To assess this, dissolved Ba concentration and isotope compositions for surface seawaters from the Siberian Shelf

and the Bering Sea/Strait are presented. These data constrain the Ba isotope composition of major Eurasian river inputs and Pacific water inflow and document the impact of non-conservative processes on mixing relationships between Arctic Ocean water sources.

2. Study area and samples

The Siberian shelves, notably the Kara, Laptev and East Siberian Seas, receive ~60% of the total riverine freshwater inputs to the Arctic Ocean (Dickson et al., 2007), ~80% of which is supplied by the rivers Yenisey (620 km^3 yr^{-1}), Lena (520 km^3 yr^{-1}) and Ob (390 km^3 yr^{-1}) (Milliman and Farnsworth, 2011) (Fig. 1). The rivers Yenisey and Ob discharge freshwater into the Kara Sea, which is transported either northwards into the Eurasian basin, mixing with seawater of Atlantic origin, or eastwards into the Laptev Sea via the Vilkitsky Strait (Janout et al., 2015, Osadchiev et al., 2020). The Lena River discharges freshwater into the Laptev Sea, which is transported either northward into the Eurasian basin, or eastwards through the East Siberian Sea and possibly the Chukchi Sea, into the Amerasian basin (Weingartner et al., 1999, Guay et al., 2001, Abrahamsen et al., 2009). Lena River water transported northwards into the Eurasian basin mixes with seawater of Atlantic origin (Abrahamsen et al., 2009). Lena River water transported eastwards into the East Siberian Sea is combined with freshwater discharged by the Kolyma (120 km^3 yr^{-1}) and Indigirka (55 km^3 yr^{-1}) rivers (Milliman and Farnsworth, 2011) and mixes with seawater of Atlantic and Pacific origin (Weingartner et al., 1999). These different transport pathways of freshwater input from these major Eurasian rivers are driven by changes in the local wind fields, often associated with pan-Arctic changes in

atmospheric circulation regime (Guay et al., 2001, Johnson and Polyakov, 2001, Steele and Ermold, 2004, Dmitrenko et al., 2005, Thibodeau et al., 2014, Janout et al., 2015, Osadchiev et al., 2020), and are invoked to play an important role in large-scale changes in Arctic Ocean freshwater distributions (Morrison et al., 2012).

Surface seawater samples (1 to 8 m depth) analyzed in this study were collected from the Kara Sea, Laptev Sea, East Siberian Sea and Chukchi Sea during the International Siberian Shelf Study (ISSS-08; August to September, 2008) on board the H/V Yacob Smirnitskyi (Alling et al, 2010) (Fig. 2). Three additional surface seawater samples (4 to 5.1 m depth) from the Bering Sea/Strait collected during the GEOTRACES GN01 section cruise (August to October, 2015) on board the USCGC Healy were also analyzed. These samples capture the mixing of freshwater discharged by the rivers Yenisey, Lena and Ob, with Atlantic and Pacific seawater. In addition a sample of Lena River water, collected in June, 2013 was also analyzed for Ba concentration and isotope composition.

In detail, 29 samples spanning the Laptev Sea, East Siberian Sea and Chukchi Sea were measured for Ba concentrations, with a subset of 17 measured for Ba isotope compositions. They encompass a gradient in salinity from 1.3 proximal to the Lena River delta, increasing to 20.66 northwards across the Laptev Sea, and to 30.66 eastwards across the East Siberian Sea and Chukchi Sea. Oxygen isotope data suggest these surface water salinity gradients predominantly reflect the mixing between Lena River freshwater and seawater, rather than salinity variations induced by sea-ice formation/melt (Rosén et al., 2015). These salinity gradients trace the transport and mixing of two plumes of Lena River freshwater; northwards across the Laptev Sea and eastwards into the East Siberian Sea and Chukchi Sea (Alling et al., 2010) (Fig. 1, Fig. 2).

Two samples collected in the Kara Sea are influenced by freshwater discharge from the rivers Ob and Yenisey with salinities 7.85 and 7.33 were analyzed for Ba concentration and isotope composition (Fig. 2). As were three surface seawater samples collected from the Bering Sea and Strait to assess the Ba concentration and isotope composition of inflowing Pacific water.

During the ISSS-08 cruise, surface seawater samples were collected by either pumping through acid-cleaned silicon tubing that was extended 10 m in front of the ship using a glass-fiber flag pole or using metal-free GO-Flo sampling bottles. They were subsequently filtered (0.22 μm Millipore nitrocellulose membrane filters) into acid-cleaned sample bottles and acidified to pH 2 using distilled HCl (SeaStar) (Lambelet et al., 2013). During the GEOTRACES GN01 section cruise the 3 surface seawater samples from the Bering Sea and Strait were collected using Niskin bottles mounted on a stainless steel rosette. They were filtered using Supor Acropak 500 capsule filters (0.45μm) into acid-cleaned low-density polyethylene cubitainers and acidified to pH 1.6 using distilled 6M HCl. The Lena River water sample was filtered (0.22 μm Millipore nitrocellulose membrane filters) into acid cleaned high density polyethylene bottles, and acidified to pH < 2 using distilled HCl (SeaStar).

3. Analytical techniques

The Ba isotope compositions of waters were determined using thermal ionization mass spectrometry (TIMS; TRITON instrument, Thermo Scientific), and a previously described double spike technique to correct for instrumental mass bias (Hsieh & Henderson, 2017). Sample aliquots of 50 ml were accurately weighed and equilibrated with a known quantity of a ^{135}Ba-^{137}Ba double spike solution. The Lena

River water sample was evaporated to dryness and refluxed in 15 M HNO_3 to digest any organic material. For all other samples, Ba was pre-concentrated by co-precipitation with $CaCO_3$ through the addition of 3ml 0.9 M Na_2CO_3 solution, which was pre-cleaned following protocols described by Hsieh & Henderson (2017). Samples with salinities <20 were first partially evaporated to increase their salinities to about 30, while samples with salinities >20 were subject co-precipitation directly. The $CaCO_3$ precipitates were separated by centrifugation, washed in 15 ml MilliQ water, dissolved in 1 ml 3M HCl and processed through a cation exchange chromatography procedure (Supplementary Table 1). The eluted Ba fractions were dried and any organics that were leached from the cation exchange resin were oxidized prior to TIMS analyses by addition and evaporation of 15 M HNO_3 and 9.8 M H_2O_2. The procedural blanks were determined to be 0.05 – 3.62 ng of Ba (n = 2, total range) representing <1.4% of the Ba processed in the samples.

Barium isotope measurements using TIMS featured a double Re filament assembly following previously described protocols (Hsieh & Henderson, 2017, Bridgestock et al., 2019). Barium isotope compositions are expressed as $\delta^{138/134}$Ba values (eqn. 1) relative to the standard reference material NIST 3104a:

$$\delta^{138/134}\text{Ba} \text{‰} = (^{138}\text{Ba}/^{134}\text{Ba}_{\text{sample}}/^{138}\text{Ba}/^{134}\text{Ba}_{\text{NIST3104a}} - 1) \times 1000 \quad (1)$$

Repeat measurements of NIST 3104a over a period of 12 months, run at ion beam intensities (6 – 10 V on ^{138}Ba, collected using Faraday cups equipped with 10^{11} Ω resistors) comparable to the majority of sample analyses, yielded a reproducibility of ± 0.03 ‰ (2SD, n = 12). This is taken to represent the level of uncertainty for Ba isotope analyses of the samples. Measurements of a secondary inter-laboratory $BaSO_4$

standard, NBS-127 yielded $\delta^{138/134}$Ba = -0.29 ± 0.02 ‰ (mean ± 2SD, n = 14), in agreement with published values ($\delta^{138/134}$Ba = -0.27 ± 0.02 ‰; Horner et al., 2017, -0.29 ± 0.01 ‰; Crockford et al., 2019, -0.28± 0.04 ‰; Tian et al., 2019, and -0.29± 0.03 ‰; Tieman et al., 2020).

Barium concentrations were obtained from the isotopic analyses by isotope dilution. Barium concentrations of samples from the ISSS-08 cruise, including an additional 12 samples that were not analyzed for Ba isotope compositions, were also determined using a quadrupole ICP-MS (PerkinElmer NexION 350D), in conjunction with a flow injection sample introduction system (Elemental Scientific prepFAST FIAS). Samples were diluted in-line by the prepFAST by a factor of 3, and spiked with a known quantity of indium that was used as an internal standard to normalize for drift in instrument sensitivity. Repeat analyses of two in-house seawater standards yielded reproducibilities better than 4% (2SD), with values in excellent agreement with those previously published (Supplementary Table 2; Hsieh & Henderson, 2017, Bridgestock et al., 2018). The accuracy of these measurements was further validated by measurement of the certified reference material, SLRS-6 (river water), with results within 4% of the consensus value (Supplementary Table 2). Barium concentrations determined by ICP-MS agree within 5% of those determined by isotope dilution from the isotopic analyses, with the exception of single sample that agrees within 26% (Supplementary Fig. 1). The isotope dilution data are considered to be more reliable so are presented and discussed in the following where available.

Dissolved Ba concentration and $\delta^{138/134}$Ba data produced for surface seawater samples from stations 1, 3 and 5 of the GEOTRACES GN01 section cruise by another laboratory (Whitmore et al., in revision, Shiller and Horner, 2021) agree within 12% and 0.05 to 0.13 ‰ of those presented in this study (Supplementary Information).

4. Results

Dissolved Ba concentrations are highest proximal to the Lena delta (209 nmol kg^{-1}) at salinity 2.7, and generally decrease with increasing salinity to 38 – 70 nmol kg^{-1} (Fig. 2, Table 1). Two distinct relationships between dissolved Ba concentration and salinity are observed (Fig. 3a,b). Samples from the Lena River freshwater plume extending eastward into the East Siberian Sea, along with the sample proximal to the Lena delta, define a negative correlation ($r^2 = 0.82$) with salinity, with a y-intercept of 197 ± 27 nmol kg^{-1} of Ba. Three samples from close to the mouth of the Kolyma River plot above this relationship and are excluded from the regression. The three seawater samples from the Bering Sea and Strait lie on this relationship with salinities of 31.8 to 32.9, and Ba concentrations of 34.7 to 54.2 nmol kg^{-1}. Samples in the freshwater plume extending northwards across the Laptev Sea, and two samples from the Buor-Khaya Gulf define a separate negative correlation with salinity ($r^2 = 0.89$) featuring a y-intercept half of that defined by the eastward plume (100 ± 11 nmol kg^{-1} of Ba). The Ba concentration of the Lena River water sample collected in June, 2013, by comparison, is 85.5 nmol kg^{-1}, which is within range of data for samples collected in month of June between 2004 and 2016 (77 to 119 nmol kg^{-1}; total range, n = 11; Cooper et al., 2008, Holmes et al., 2021). Kara Sea surface water samples proximal to the mouths of the Ob and Yenisey feature Ba concentrations of 93.2 and 49.9 nmol kg^{-1}, respectively.

Dissolved $\delta^{138/134}$Ba increase with salinity from 0.2 to 0.3 ‰ up to 0.55 ‰ in the Bering Sea/Strait (Fig, 2c, 3c, 3d, Table 1). As with dissolved Ba concentrations, the samples transecting northward across Laptev Sea and from the Buor-Khaya Gulf

define a different relationship between $\delta^{138/134}$Ba and salinity than those from the Lena River water plume spreading eastward into the East Siberian Sea and Chukchi Sea (Fig. 3c,d). Specifically the former increases to maximum $\delta^{138/134}$Ba at lower salinities (~20) that the latter. Samples from the Bering Sea/Strait lie on the $\delta^{138/134}$Ba – salinity relationship defined by samples from the eastward spreading Lena River water plume. These two groups of samples also display linear correlations between $\delta^{138/134}$Ba and 1/Ba concentration (r^2 = 0.70 and 0.89; Fig. 4). The Lena River water sample features $\delta^{138/134}$Ba of 0.27 ± 0.03 ‰ in good agreement with the value published by Cao et al. (2020a) of 0.32 ± 0.04 ‰.

5. Discussion

5.1 Constraints on the Ba concentration and $\delta^{138/134}$Ba of major Eurasian river inputs to the Arctic Ocean

The Yenisey (620 km^3 yr^{-1}), Lena (520 km^3 yr^{-1}) and Ob (390 km^3 yr^{-1}) are the three largest rivers in terms of supplying freshwater to the Arctic Ocean, representing ~80% of total Eurasian river discharge (Dickson et al., 2007, Milliman and Farnsworth, 2011) (Fig. 1). To estimate the Ba concentrations and $\delta^{138/134}$Ba of freshwater input from these rivers, mixing relationships between these variables and salinity are extrapolated to salinity 0 (Fig. 3, Fig. 4, Fig. 5; Supplementary Information). This yields an estimate of the 'effective' river endmember, which accounts for the Ba flux transported by the river dissolved load, and its modification by estuarine processes, notably due to desorption of Ba from exchangeable sites on riverine suspended sediments (e.g. Hanor and Chan, 1977). These effective river

endmember values are then used to estimate the average Ba concentration and $\delta^{138/134}$Ba of Eurasian riverine freshwater inputs to the Arctic Ocean (section 5.1.3). We note however that the effective river endmember values for the rivers Yenisey and Ob are based on limited data, and should consequently be treated with caution (section 5.1.2).

5.1.1 Constraints on the Ba concentration and $\delta^{138/134}$Ba of Lena River freshwater inputs

Samples from the Laptev, East Siberian and Chukchi seas define two distinct mixing relationships between salinity, Ba concentration and $\delta^{138/134}$Ba (Fig. 3, Fig. 4). These mixing relationships correspond to different transport pathways of the Lena River freshwater plume; eastwards into the East Siberian Sea and Chukchi Sea, and northwards across the Laptev Sea (Alling et al., 2010, section 2). In the East Siberian Sea, three samples collected proximal to the mouth of the Kolyma River deviate from the Ba concentration-salinity mixing relationship defined by the eastward Lena River freshwater plume, likely due to input of freshwater from the Kolyma River (Fig. 2, Fig. 3). For this reason they have been excluded from the regressions used to estimate the effective river Ba concentration of the eastward Lena River plume. Mixing relationships defined by samples from the eastward and northward Lena River plumes yield different effective river Ba concentrations and $\delta^{138/134}$Ba values of 197 ± 27 nmol kg^{-1} and 0.20 ± 0.06 ‰, and 100 ± 11 nmol kg^{-1} 0.25 ± 0.05 ‰, respectively (Table 2). These effective river Ba concentrations are in general agreement with that previously published of 134 ± 43 nmol kg^{-1} based on sampling in August/September, 1995 (Guy and Falkner, 1998, Supplementary Figure 2).

The differences in effective river endmember values for the northward and eastward Lena River plumes are interpreted to represent temporal variations in the Ba concentration and $\delta^{138/134}$Ba values of Lena River freshwater inputs. The northward versus eastward transport of Lena River freshwater is driven by changes in prevailing wind direction (Johnson and Polyakov, 2001, Steele and Ermold, 2004, Dmitrenko et al., 2005, Thibodeau et al., 2014) (Fig. 1). In 2008 (the year of sample collection) the prevailing wind direction favored the northward transport of Lena River freshwater across the Laptev Sea (Wegner et al., 2013, Thibodeau et al., 2014). The freshwater in this transect of the ISSS-08 cruise is interpreted to represent Lena River water discharged within the ~2 months proceeding sample collection (i.e. July – August, 2008; Alling et al., 2010). In contrast, in 2007 (the year prior to sample collection) the prevailing wind direction favored the eastward transport of Lena River freshwater into the East Siberian Sea (Wegner et al., 2013, Thibodeau et al., 2014). The residence time of riverine freshwater in this region is estimated to be several years (Schlosser et al., 1994, Alling et al., 2010), and so mixing relationships defined by eastward plume likely reflects Lena River discharge integrated over multiple years.

The flux and isotope composition of dissolved Ba from river catchments to the ocean is commonly modified in estuaries, predominantly due to release of exchangeable Ba from riverine suspended particles (Hanor and Chan, 1977, Guay and Falkner, 1998, Bridgestock et al., 2021). The effective river Ba concentrations estimated for the eastward Lena River plume (197 ± 27 nmol kg^{-1}) is significantly higher than the discharged weighted average Ba concentration of the Lena River dissolved load of 104 nmol kg^{-1} (n = 56) based on multi-year time-series data spanning 2003 to 2016 (Cooper et al., 2008, Holmes et al., 2021). This suggests that about half of the Ba content of Lena River freshwater in the eastward plume is

derived from estuarine processes. In contrast the effective river Ba concentrations estimated for the northward Lena River plume (100 ± 11 nmol kg^{-1}) is within uncertainty of the average Ba concentrations of the Lena River dissolved load in July-August (96 ± 22 nmol kg^{-1}; mean ± 2sd) and the discharge weighted multi-year average (104 nmol kg^{-1}; Cooper et al., 2008, Holmes et al., 2021). This suggests negligible modification of the Ba concentration of freshwater transported by the northward Lena River plume by estuarine processes.

Release of particulate Ba in estuaries has recently been shown to lower the $\delta^{138/134}$Ba of net riverine Ba fluxes to the ocean, relative to the dissolved load (Bridgestock et al., 2021). Data for Lena River dissolved load $\delta^{138/134}$Ba is only available for summer months featuring 0.27 ± 0.03 ‰ (June, 2013; this study) and 0.32 ± 0.04 ‰ (August, 2011; Cao et al., 2020a). These values are in agreement with the effective $\delta^{138/134}$Ba of the northward Lena River plume of 0.25 ± 0.05 ‰, consistent with the inferred negligible modification of the Lena River Ba flux by estuarine processes. These values are, however, slightly higher that the effective river $\delta^{138/134}$Ba of the eastward Lena River plume of 0.20 ± 0.06 ‰ (Fig. 3). This offset could partially represent seasonal variability in the Lena River dissolved load $\delta^{138/134}$Ba that is not characterized by the available data. It is, however, also consistent with observations from the estuaries of the Amazon, Fly and Johor rivers, that estuarine release of dissolved Ba decreases the $\delta^{138/134}$Ba of riverine freshwater inputs to the ocean (Bridgestock et al., 2021). These observations are interpreted to be caused by the release of isotopically light Ba from exchangeable sites on riverine suspended particles, due to exchange with major cations in seawater (Bridgestock et al., 2021).

It is unclear what controls the large difference in estuarine Ba release inferred for the northward and eastward Lena River plumes (Fig. 3). This could reflect temporal changes in the suspended sediment concentration of freshwater discharged to the Laptev Sea by the Lena River, and/or the cation exchange capacity of the suspended sediment, which are likely to be key controls on the magnitude of estuarine Ba release (e.g. Bridgestock et al., 2021). Wegner et al. (2013) studied the distribution of suspended particulate matter in the Laptev Sea proximal to the Lena River delta in the summers of 2007 and 2008, corresponding to the time periods relevant for freshwater discharge for the eastward and northward Lena River plumes respectively. Suspended particulate and Lena River freshwater distributions were strongly linked, and suspended particulate concentrations were generally lower in 2008 (corresponding to the northward Lena River water plume), than 2007 (corresponding to the eastward Lena River water plume) (Wegner et al., 2013). These observations are qualitatively consistent with difference in magnitude in estuarine release between these different Lena River water plumes. Whatever the cause, these large temporal variations in effective river Ba concentrations for Lena River freshwater represent a source of uncertainty for using dissolved Ba concentrations to quantify Arctic Ocean water sources.

5.1.2 Constraints on the Ba concentration and $\delta^{138/134}$Ba of Yenisey and Ob River freshwater inputs

The two samples collected proximal to the mouths of the rivers Yenisey and Ob permit rudimentary estimates of the effective Ba concentration and $\delta^{138/134}$Ba of these major Eurasian rivers (Fig. 2). It is assumed that freshwater discharged from

these rivers mixes with seawater of Atlantic origin featuring a salinity, Ba concentration and $\delta^{138/134}$Ba of 34.92, 43 ± 3 nmol kg^{-1} (Guay et al., 2009) and 0.53 ± 0.06 ‰, respectively (Table 3), and that the salinity of these samples has not been significantly modified by sea ice formation/melt. The $\delta^{138/134}$Ba of Atlantic-derived seawater is constrained using a compilation of North Atlantic surface water (<100 m) data (Hsieh and Henderson, 2017, Bates et al., 2017, Bridgestock et al., 2021), the details of which are provided in the Supplementary Information file (Supplementary Table 4). Extrapolation of conservative mixing relationships between this Atlantic seawater endmember and data for the two Kara Sea samples yield effective river Ba concentrations and $\delta^{138/134}$Ba of 52 ± 4 nmol kg^{-1} and 0.31 ± 0.04 ‰ for the Yenisey River, and 108 ± 6 nmol kg^{-1} and 0.23 ± 0.04 ‰ for the Ob River (Fig. 5). Uncertainties on these values are estimated by propagation of uncertainties on the measured Ba concentration and $\delta^{138/134}$Ba of the samples (± 5 % and ± 0.03 ‰; 2sd), and those assigned for Atlantic derived seawater (± 7 % and ± 0.06 ‰; 2sd), using Monte Carlo methods. These values, however, may be subject to additional systematic errors related to the assumptions stated above that are difficult quantify and so should be treated with a degree of caution. In particular, the Kara Sea is an area of pronounced seasonal sea ice formation and melting (Bauch et al., 2003), which would alter the salinity of the samples and hence the Ba concentration/ $\delta^{138/134}$Ba – salinity mixing relationships. Unfortunately oxygen isotope data are not available for the Kara Sea samples that would be required to assess this.

The calculated effective river Ba concentrations are comparable to those determined from samples collected in 1994/1995 of 63 ± 40 nmol kg^{-1} and 91 ± 12 nmol kg^{-1} for the rivers Yenisey and Ob respectively (Guy and Falkner, 1998; Supplementary Figure 3). They are also in good agreement with the discharged

weighted average Ba concentrations of the Yenisey (59 nmol kg^{-1}) and Ob (117 nmol kg^{-1}) dissolved loads (Fig. 5), based on multi-year time-series data spanning 2003 to 2016 (Cooper et al., 2008, Holmes et al., 2021). This suggests that estuarine processes play a negligible role in modifying the Ba concentration of freshwater discharged by these rivers to the Kara Sea, at least during the studied time period. However, given the limited data and above stated assumptions used to estimate the effective river endmember Ba concentrations, this assertion should be treated with caution.

5.1.3 Estimate of the average Ba concentration and $\delta^{138/134}$Ba of Eurasian freshwater inputs to the Arctic Ocean

The effective river Ba concentrations determined for the rivers Yenisey, Lena and Ob are weighted by the annual average discharges of these rivers, of 620 km^3 yr^{-1}, 520 km^3 yr^{-1} and Ob 390 km^3 yr^{-1} respectively (Milliman and Farnsworth, 2011) to estimate an average Ba concentration of Eurasian river freshwater inputs to the Arctic Ocean of 116 ± 9 nmol kg^{-1} (Table 3). This is comparable to previous estimates of 130 ± 20 nmol kg^{-1} (Guy and Falkner, 1998) and 158 nmol kg^{-1} (Charette et al., 2020), based on sampling of major Eurasian river estuaries and the Eurasian river water within the Transpolar Drift, respectively. Likewise, the effective river $\delta^{138/134}$Ba values of these three rivers are weighted by their effective river Ba concentrations and annual average discharges to estimate an average $\delta^{138/134}$Ba of Eurasian river freshwater inputs to the Arctic Ocean of 0.23 ± 0.04 ‰. Effective river endmember values for the eastward Lena River plume are selected to represent of those for the Lena River for calculation of these averages, rather than those for the northern Lena River plume. This is because the former are interpreted to represent the average of

several years of Lena River freshwater discharge, compared to several months for the later (section 5.1.1). Uncertainties on these values were calculated by propagating uncertainties (2sd) on effective Ba concentration and $\delta^{138/134}$Ba of the individual rivers using Monte Carlo methods. There are, however, additional sources of uncertainty in how representative these values are for average Eurasian river freshwater input in the Arctic Ocean, which are hard to assess without more data. Notably, temporal variability in the effective Ba concentration and $\delta^{138/134}$Ba of the rivers Yenisey, Lena and Ob (as noted in section 5.1.1), and how well they represent those of freshwater input from the other smaller rivers that contribute ~20% of the Eurasian riverine freshwater input to the Arctic Ocean (Dickson et al., 2007, Milliman and Farnsworth, 2011). These uncertainties aside, these values represent initial constraints on the $\delta^{138/134}$Ba of Eurasian freshwater inputs to the Arctic Ocean.

5.2 Systematically higher effective river $\delta^{138/134}$Ba values of major Arctic Eurasian rivers relative to other rivers and rocks

The effective river $\delta^{138/134}$Ba values estimated for the rivers Yenisey, Lena and Ob (0.20 to 0.31 ‰) are higher than those available for other rivers, the Amazon (0.01 ± 0.06 ‰), Paraná-Uruguay (0.03 ± 0.09 ‰), Fly (0.11 ± 0.06 ‰) and Johor (0.06 ± 0.12 ‰) (Hsieh and Henderson, 2017, Bridgestock et al., 2021). The latter are consistent with the composition of the upper continental crust (0.00 ± 0.04 ‰; Nan et al., 2018), representing the expected average composition of Ba released by chemical weathering of rocks in these catchments. The cause of the higher effective $\delta^{138/134}$Ba values for the major Arctic rivers presented in this study is unclear but could reflect unusually high $\delta^{138/134}$Ba of rocks within these catchments, or that a reservoir of

isotopically light Ba is either accumulating within soils in these catchments or is being exported bound within non-exchangeable sites of secondary minerals and/or organic matter.

A significant fraction of the sediment mobilized in the catchments of the rivers Yenisey, Lena and Ob is not transported through the estuarine mixing zones, and is instead deposited within the flood plains/deltas of these river systems, or is trapped by dams (Meade et al. 2000, Fedorova et al. 2015). This could potentially explain the higher $\delta^{138/134}$Ba of the effective endmembers of these rivers, compared to those for other rivers and rocks. A large fraction of the Ba released by chemical weathering is adsorbed to the surfaces of secondary minerals (e.g. Nesbitt et al., 1980), which gets transported by suspended sediment loads and ultimately released by into the dissolved phases within estuaries due to exchange with major cations in seawater (e.g. Hanor and Chan, 1977). Recent studies have proposed Ba adsorption to secondary minerals within river catchments is associated with an isotope fractionation favoring the lighter Ba isotopes (low $\delta^{138/134}$Ba), resulting in an enrichment of heavier Ba isotopes (high $\delta^{138/134}$Ba) in river dissolved loads relative to the weathering lithology (Gong et al., 2020, Gou et al. 2020). The release of this Ba adsorbed to suspended river sediments in estuaries elevates effective river Ba concentrations and decreases effective river $\delta^{138/134}$Ba relative to those of river dissolved loads (Bridgestock et al., 2021). The deposition of suspended sediment within these river catchments, rather than its transport through the estuarine mixing zones, would therefore be expected to result in the accumulation a reservoir adsorbed Ba featuring low $\delta^{138/134}$Ba, increasing the $\delta^{138/134}$Ba of the effective river values. More data is required to validate this hypothesis, but it would suggest that Ba isotopes could prove to be a useful tracer of sediment mobilization and deposition within river catchments.

5.3 Modification of dissolved Ba concentration and $\delta^{138/134}$Ba of Lena River freshwater exported to the Eurasian basin by non-conservative processes

Non-conservative processes can modify mixing relationships between riverine freshwater and Arctic Ocean seawater, impacting the utility of dissolved Ba concentrations to trace these water sources (Guay and Falkner, 1997, Abrahamsen et al., 2009, Thomas et al., 2011, Roeske et al., 2012, Hendry et al., 2018). To assess the potential impact of such processes, the Lena River freshwater plume mixing relationships are used to predict Arctic Ocean seawater Ba concentrations and $\delta^{138/134}$Ba, which are compared to independent constraints for these water sources.

Arctic Ocean seawater is derived from inflow of Atlantic and Pacific seawater (Fig. 1). Atlantic-derived seawater features a salinity of 34.92 and Ba concentration of 43 ± 3 nmol kg^{-1} (Roeske et al., 2012, Guay et al., 2009) (Table 3). The $\delta^{138/134}$Ba of Atlantic-derived water in the Arctic Ocean is constrained by literature data for North Atlantic surface seawater (< 100 m), which displays a homogeneous $\delta^{138/134}$Ba of 0.53 ± 0.06 ‰ (Bates et al., 2017, Hsieh and Henderson, 2017, Bridgestock et al., submitted) (Supplementary Table 4). Pacific-derived water features a lower salinity and higher Ba concentration of 32.7 and 55 ± 5 nmol kg^{-1} (Guay et al., 2009; Table 3), reflecting the input of riverine freshwater prior to transport through the Bering Strait (Fig. 1). The sample collected in the Bering Strait reported in this study is used to constrain the $\delta^{138/134}$Ba of Pacific-derived water to be 0.55 ± 0.03 ‰. This sample has a salinity and Ba concentration of 32.2 and 54.2 nmol kg^{-1} in good agreement with endmember values reported by previous studies for this water source (Guay et al., 2009).

Lena River water transported eastward likely mixes with both Atlantic- and Pacific-derived seawater (Weingartner et al., 1999) (Fig. 1). Extrapolating the mixing relationships defined by eastward Lena River freshwater plume to the salinities Atlantic- and Pacific-derived seawater predict Ba concentrations and $\delta^{138/134}$Ba values (Table 2) that are within uncertainty of the endmember values for these water sources (Table 3, Fig. 3, Fig. 4). This is consistent with conservative behavior of dissolved Ba concentrations and $\delta^{138/134}$Ba during mixing between Lena River water and Arctic Ocean seawater. The uncertainty on the Ba concentrations and $\delta^{138/134}$Ba predicted for these water sources by the mixing relationships are, however, large; so non-conservative processes could potentially modify Ba concentrations and $\delta^{138/134}$Ba by up to 65 % and 0.4 ‰ respectively, without being resolved by this data.

Lena River water transported northward mixes with Atlantic-derived seawater (Abrahamsen et al., 2009) (Fig. 1). Extrapolation of the relationships defined by northward Lena River freshwater plume to the salinity of Atlantic-derived seawater predicts a Ba concentration of 28 ± 22 nmol kg^{-1} and a $\delta^{138/134}$Ba of 0.88 ± 0.28 ‰ (Table 2). This predicted Ba concentration is within uncertainty of the endmember value for Atlantic-derived water of 43 ± 3 nmol kg^{-1} (Table 3), although the large uncertainty on the predicted value means non-conservative processes could potentially modify Ba concentration of this endmember by up to ~86 %. The predicted $\delta^{138/134}$Ba for Atlantic-derived seawater however is significantly higher (i.e. outside of uncertainty) than the endmember value for Atlantic-derived water of 0.53 ± 0.06 ‰. In fact it is significantly higher than any seawater $\delta^{138/134}$Ba value measured to date (Horner et al., 2015, Bates et al., 2017, Hsieh and Henderson, 2017, Bridgestock et al., 2018, Geyman et al., 2019, Cao et al., 2020a, Cao et al., 2020b).

Sea-ice melting could modify the observed mixing relationships, but would be required to decrease the salinity of Atlantic-derived seawater to ~25 to explain the difference between the predicted and endmember $\delta^{138/134}$Ba of this water source. Although we note that the impact of sea-ice melting (or formation) on seawater $\delta^{138/134}$Ba values is unknown, and it remains uncertain how exactly these processes impact salinity-dissolved Ba concentration relationships (Hendry et al., 2018). The Laptev Sea is an important area for net sea ice formation, and oxygen isotope data for this transect of the cruise show no resolvable impact of sea-ice melting (Rosén et al., 2015). Sea ice melting is therefore unlikely to explain the observed difference between the predicted and endmember $\delta^{138/134}$Ba of Atlantic-derived seawater along the Laptev Sea shelf break. Instead these differences are interpreted to reflect the non-conservative removal of dissolved Ba from the surface ocean with an associated isotope fraction.

Abrahamsen et al. (2009) and Roeske et al. (2012) documented depletions of surface water dissolved Ba concentrations of between 35 to 40% along the shelf break of the Laptev Sea in 2007 (the year prior to sample collection in this study) compared to those predicted by conservative mixing between Eurasian river freshwater and Arctic seawater. The magnitude of these Ba depletions agree with the average Ba depletion of 35 ± 53 % implied by the comparison between the predicted (28 ± 22 nmol kg^{-1}; for the northern Lena River freshwater plume) and endmember (43 ± 3 nmol kg^{-1}) values for Atlantic-derived seawater (Table 2, Table 3). The uncertainty on this value is however large, but this agreement with the magnitudes of non-conservative Ba depletions found by other studies for the same region and similar time period, lends confidence to the inference that such processes have modified the $\delta^{138/134}$Ba of Atlantic-derived seawater in this region.

The removal of dissolved Ba and accompanying increases in $\delta^{138/134}Ba$ can be explained by batch (eqn. 2) or Rayleigh (eqn. 3) isotope fractionation models (Fig. 6).

$$\delta^{138/134}Ba_{predcited} = \delta^{138/134}Ba_{endmember} + [1000 \times (\alpha_{diss/part} - 1)] \times f_{removed} \quad (2)$$

$$\delta^{138/134}Ba_{predicted} = \delta^{138/134}Ba_{endmember} - [1000 \times (\alpha_{diss/part} - 1)] \times \ln(1 - f_{removed}) \quad (3)$$

Where $f_{removed}$ denotes the fraction of dissolved Ba removed relative to the endmember concentrations for Atlantic-derived seawater (0.35 ± 0.53), and $\delta^{138/134}Ba_{predicted}$ and $\delta^{138/134}Ba_{endmember}$ denote the isotope composition predicted (0.88 ± 028 ‰) and endmember values for Atlantic-derived seawater (0.53 ± 0.06 ‰). The isotope fractionation factor, $\alpha_{diss/part}$, is defined as the $^{138}Ba/^{134}Ba$ ratio of dissolved Ba ($_{diss}$), relative to the $^{138}Ba/^{134}Ba$ ratio of particulate Ba ($_{part}$).

Previous studies have constrained $\alpha_{diss/part}$ to be ≈1.0005 in open ocean settings (Hsieh and Henderson, 2017, Horner et al., 2017, Bridgestock et al., 2018, Cao et al., 2020b), attributed to $BaSO_4$ formation associated with the production and export of organic matter. While a $\alpha_{diss/part}$ of 1.0005 can explain the predicted Atlantic-derived seawater $\delta^{138/134}Ba$ values ($\delta^{138/134}Ba_{predicted}$) within the uncertainty on $\delta^{138/134}Ba_{predicted}$ and $f_{removed}$, a higher $\alpha_{diss/part}$ of 1.001 provides the best fit to $\delta^{138/134}Ba_{predicted}$ using either a batch (eqn. 2) or Rayleigh (eqn. 3) fractionation model (Fig. 6). It is possible that the observed Ba depletion along the Laptev Sea shelf break is the result of non-conservative processes other than $BaSO_4$ formation and is associated with a different isotope fractionation factor. For example, Roeske et al. (2012) suggested that the Ba depletion observed in this location in 2007 could be due to scavenging by terrestrial organic matter. The large uncertainty on $\delta^{138/134}Ba_{predicted}$ and $f_{removed}$, however,

preclude any firm conclusions regarding the mechanisms of Ba removal and the magnitude of associated isotope fractionation along the margin of the Siberian Shelf at this stage. Improved constraints on these mechanisms and isotope fractionation factors will be important for assessing the use of Ba isotopes to trace riverine freshwater in the Arctic Ocean (section 5.5).

More generally, these results highlight the potential importance of such processes for modifying the $\delta^{138/134}$Ba of riverine inputs to open ocean settings. Previous studies have shown that Ba removal in high salinity regions of estuarine mixing zones, similar to that inferred in this study along the Laptev Sea shelf break, can be important for modifying net riverine Ba fluxes to the ocean (e.g. Stecher and Kogut, 1999, Nozaki et al., 2001). Understanding importance of such processes at a global scale, and their impact on the $\delta^{138/134}$Ba of riverine inputs to open ocean settings is needed to fully realize the potential of Ba isotopes as an emerging tracer of marine processes.

5.4 Implications for using Ba concentrations and $\delta^{138/134}$Ba to trace riverine freshwater transport within the Arctic Ocean

Modification of Arctic Ocean dissolved Ba inventories by non-conservative processes, as inferred in this study along the Laptev Sea shelf break, represents a major issue for applying dissolved Ba concentrations to trace riverine freshwater transport pathways within the Arctic Ocean (Guy and Falkner, 1997, Abrahamsen et al., 2009, Roeske et al., 2012). Barium isotopes could potentially provide additional constraints to distinguish between roles of mixing and non-conservative processes for setting Arctic Ocean dissolved Ba distributions, improving the reliability of Ba as a

tracer of riverine freshwater sources to the Arctic Ocean. The utility of this approach depends on the specific dissolved Ba concentration-$\delta^{138/134}$Ba relationships that result from mixing between Arctic Ocean water sources, and from non-conservative processes that cycle Ba in the Arctic Ocean. Optimal constraints would be provided if these relationships were orthogonal to each other. Processes that deplete dissolved Ba concentrations inferred in this study, however, result in Ba concentration and $\delta^{138/134}$Ba changes that are roughly parallel to mixing relationships between average Eurasian riverine freshwater and unmodified Atlantic and Pacific derived seawater (Fig. 7). Notably, mixing relationships between Eurasian river water and Arctic Ocean seawater are indistinguishable from the global relationship between seawater Ba concentration and $\delta^{138/134}$Ba, which arises from a combination of large-scale water mass mixing and non-conservative Ba cycling between the surface and deep ocean (Horner et al. 2015, Bates et al., 2017, Hsieh and Henderson, 2017, Bridgestock et al. 2018). This unfortunately limits the ability of coupled measurements of dissolved Ba concentration and $\delta^{138/134}$Ba to discern between the impact of mixing and non-conservative processes.

Despite the issues stated above, coupled measurements of dissolved Ba concentration and $\delta^{138/134}$Ba could yet prove useful for constraining conservative versus non-conservative controls on Arctic Ocean Ba distributions. Firstly, the exact magnitude of the isotope fractionation accompanying non-conservative Ba removal along the Arctic Ocean margin remains poorly constrained (Fig. 6). Through improved constraints on the isotope fractionation factors, this approach could yet still prove to be viable, especially if the magnitude of the isotope fractionation proves to be large (i.e. $\alpha_{diss/part} \approx 1.001$), as this would result in some ability to discern between Ba concentration- $\delta^{138/134}$Ba relationships resulting from mixing versus non-

conservative processes (Fig. 7). Secondly, constraints for the $\delta^{138/134}$Ba for North American riverine freshwater inputs are currently lacking (Table 3). Barium concentration- $\delta^{138/134}$Ba mixing relationships between Arctic Ocean seawater and this important Arctic Ocean freshwater source could transpire to be clearly distinguishable from those arising from non-conservative processes. Furthermore, data constraining the fluxes and $\delta^{138/134}$Ba of benthic and submarine groundwater Ba inputs along the Arctic Ocean continental shelves are needed to assess the potential importance of such sources on Arctic Ocean dissolved Ba inventories.

6. Conclusions

Mixing between freshwater inputs from major Eurasian rivers, the Yenisey, Lena and Ob, and Atlantic and Pacific derived seawater are traced by relationships between salinity, Ba concentration and $\delta^{138/134}$Ba. These water sources are constrained to feature $\delta^{138/134}$Ba of 0.23 ± 0.04 ‰ (average Eurasian river freshwater), 0.53 ± 0.06‰ (Atlantic-derived seawater) and 0.55 ± 0.03 ‰ (Pacific-derived seawater). Non-conservative processes are inferred to modify these mixing relationships along the Laptev Sea shelf break, with an associated isotope fractionation of similar magnitude to that constrained in open ocean settings. These processes result in Ba concentration-$\delta^{138/134}$Ba relationships that are parallel to those resulting from mixing between Eurasian river freshwater and Arctic Ocean seawater, which limits utility of Ba isotopes to improve the reliability of dissolved Ba inventories to trace Arctic Ocean riverine freshwater transport pathways. More generally, the results of this study advance understanding of the cycling of Ba isotopes in the environment, and their development as an emerging tracer of marine processes.

Acknowledgements

Robert F. Anderson and Martin Q. Fleisher (Lamont-Doherty Earth Observatory of Columbia University, Palisades, New York, USA) are thanked for providing seawater samples from the Bering Sea/Strait collected during the GEOTRACES GN01 section cruise. We also thank the captains, crews, Igor Semiletov and cruise participants of the H/V Yacob Smirnitskyi during the International Siberian Shelf Study (ISSS-08; August to September, 2008), and the USCGC Healy during the GEOTRACES GN01 section cruise (August to October, 2015). The handling editor, Isaac Santos, and two anonymous reviewers are thanked for their comments that helped improve this manuscript. The ISSS-08 program was supported by the Knut and Alice Wallenberg Foundation, the Far Eastern Branch of the Russian Academy of Sciences and the Swedish Research Council (VR contract 621–e2004-4283).

Author contributions

L. B. conceived and designed the study, with input from Y-T. H., D. P. and G. M. H. Sample collection was conducted by D. P. and P. S. A. Data was produced by J. N., L. B., Y-T. H. and P. H. The manuscript was written by L. B. with input from all of the authors.

References

Aagaard, K. and Carmack, E. C., 1989, The role of sea ice and other fresh water in the Arctic Circulation, *Journal of Geophysical Research*, 94, 485-489

Abrahamsen, E. P., Meredith, M. P., Falkner, K., K., Torres-Valdes, S., Leng, K. J., Alkire, M. B., Bacon, S., Laxon, S. W., Polyakov, I. and Ivanov, V., 2009, Tracer-derived freshwater composition of the Siberian continental shelf and slope following the extreme Arctic summer of 2007, *Geophysical Research Letters,* 36, doi:10.1029/2009GL037341

Alkire, M. B., Morison, J., Schweiger, A., Zhang, J., Steele, M., Peralta-Ferriz, C. and Dickinson, S., 2017, A meteoric water budget for the Arctic Ocean, *Journal of Geophysical Research: Oceans*, doi:10.1002/2017JC012807

Alling, V., Sanchez-Garcis, L., Porcelli, D., Pugach, S., Vonk, J. E., van Dongen, B., Mörth, C-M., Anderson, L. G., Sokolov, A., Andersson, P., Humborg, C., Semiletov, I. and Gustafsson, Ö., 2010, Nonconservative behavior of dissolved organic carbon across the Laptev and East Siberian seas, *Global Biogeochemical Cycles,* 24, doi:10.1029/2010GB003834

Arrigo, K. R. and van Dijken, G. L., 2015, Continued increases in Arctic Ocean primary production, *Progress in Oceanography*, 136, 60-70, doi:10.1016/j.pocean.2015.05.002

Bates S. L., Hendry K. R., Pryer H. V., Kinsley C. K., Pyle K. M., Woodward E. M. and Horner T. J., 2017, Barium isotopes reveal role of ocean circulation on barium cycling in the Atlantic*, Geochim.Cosmochim. Acta*, 204, 286-299, doi: 10.1016/j.gca.2017.01.043

Bauch, D., Erlenkeuser, H., Stanovoy, V., Simstich, J. and Spielhagen, R. F., 2003, Freshwater distribution and brine waters in the southern Kara Sea in summer 1999 as depicted by d18O results. *In: Siberian River Run-off in the Kara Sea: Characterisation, Quantification, Variability and Environmental Significance*. , ed. by Stein, R., Fahl, K., Fütterer, D. K., Galimov, E. M. and Stepanets, O. V., *Proceedings in Marine Sciences*, 6, 73-90

Bridgestock L., Hsieh Y-T., Porcelli D., Homoky W. B., Bryan A. and Henderson G. M., 2018, Controls on the barium isotope compositions of marine sediments, *Earth and Planetary Science Letters*, 481, 101-110, doi: 10.1016/j.epsl.2017.10.019

Bridgestock L., Hsieh Y-T Porcelli D. and Henderson G. M., 2019, Increased export production during recovery from the Paleocene-Eocene thermal maximum constrained by sedimentary Ba isotopes, *Earth and Planetary Science Letters,* 510, 53-63, doi:10.1016/j.epsl.2018.12.036

Bridgestock, L., Nathan, J., Paver, R., Hsieh, Y-T. Porcelli, D., Tanzil, J., Holdship, P., Carrasco, G., Annammala, K. V., Swarzenski', P. W., and Henderson, G. M., 2021, Estuarine processes modify the isotope composition of dissolved riverine barium fluxes to the ocean, *Chemical Geology*, 579, doi:10.1016/j.chemgeo.2021.120340

Carmack., E. C., Yamamoto-Kawai, M., Haine, T. W. N., Bacon, S., Bluhm, B. A., Lique, C., Melling, H., Polyakov, I. V., Straneo, F., Timmermans, M.-L. and Williams, W. J., 2016, Freshwater and its role in the Arctic Marine System: Sources, disposition, storage, export, and physical and biogeochemical consequences in the Arctic and global oceans, *Journal of Geophysical Research: Biogeosciences,* doi:10.1002/2015JG003140

Cao, Z., Siebert, C., Hathorne, E. C., Dai, M. and Frank, M., 2020a, Corrigendum to "Constraining the oceanic barium cycle with stable barium isotopes", *Earth and Planetary Science Letters*, 530, 116003, doi:10.1016/j.epsl.2019.116003

Cao, Z., Li, Y., Rao, X., Yu, Y., Hathorne, E. C., Siebert, C., Dai, M. and Frank, M., 2020b, Constraining barium isotope fractionation in the upper water column of the South China Sea, *Geochim. Cosmochim. Acta.,* 288, 120-137, doi:10.1016/j.gca.2020.08.008

Charette, M. A., et al., 2020, The transpolar drift as a source of riverine and shelf-derived trace elements to the central Arctic Ocean, *Journal of Geophysical Research-Oceans*

Cooper L. S., McClelland J. W., Holmes R. M., Raymond P. A., Gibson J. J., Guay, C. K. and Peterson B. J., 2008, Flow-weighted values of runoff tracers ($\delta^{18}O$, DOC, Ba, alkalinity) from the six largest Arctic rivers, *Geophys. Res. Letters*, 35, doi:10.1029/2008GL035007

Crockford P. W., Wing B. A., Paytan A., Hodgskiss M. S. W., Mayfield K. K., Hayles J. A., Middleton J. E., Ahn A-S. C., Johnson D. T., Caxito F., Uhlein G., Halverson, G. P., Eickmann B., Torres M. and Horner T. J., 2019, Barium-isotopic constraints on the origin of post-Marinoan barites, *Earth and Planetary Science*, 519, 234-244, doi:10.1016/j.epsl.2019.05.018

Dickson, R., Rudels, B., Dye, S., Karcher, M., Meincke, J. and Yashayaev, I, 2007, Current estimates of freshwater flux through Arctic and subarctic seas, *Progress in Oceanography,* 73, 210-230, doi:10.1016/j.pocean.2006.12.003

Dmitrenko, I., Kirillov, S., Eicken, H. and Markova, N., 2005, Wind-driven summer surface hydrography of the eastern Siberian shelf, *Geophysical Research Letters,* 32, doi:10.1029/2005GL023022

Dodd, P. A., Heywood, K. J., Meredith, M. P., Naveira-Garabato, A. C., Marca, A. D. and Falkner, K. K., 2009, Sources and fate of freshwater exported in the East Greenland Current, *Geophysical Research Letters*, 36, doi:10.1029/2009GL039663

Ekwurzel. B., Schlosser, P., Mortlock, R. A., Fairbanks, R. G. and Swift, J. H., 2001, River runoff, sea ice meltwater, and Pacific water distribution and mean residence times in the Arctic Ocean, *Journal of Geophysical Research,* 106, 9075-9092

Fedorova, I., Chetverova, A., Bolshiyanov, D., Makarov, A., Boike, J., Heim, B., Morgenstern, A., Overduin, P. P., Wegner, C., Kashina, V., Eulenburg, A., Dobrotina, E. and Sidorina, I., 2015, Lena Delta hydrography and geochemistry: long-term hydrological data and recent observations, *Biogeosciences*, 12, 345-363, doi:10.5194/bg-12-345-2015

Geyman B. M., Ptacek J. L., LaVigne M. and Horner T. J., 2019, Barium in deep-sea bamboo corals: Phase associations, barium stable isotopes, & prospects for paleoceanography, *Earth and Planetary Science Letters*, 525, doi:10.1016/j.epsl.2019.115751

Gong, Y., Zeng, Z., Cheng, W., Lu, Y., Zhang, L., Yu, H. and Huang, F., 2020, Barium isotopic fractionation during strong weathering of basalt in a tropical climate, *Environment International*, 143**,** 105896, doi:10.1016/j.envint.2020.105896

Gou L., Jon Z., Galy A., Gong Y., Nan C. J., Wang X., Bouchez J., Cai H., Chen J., Yu H. and Huang F., 2020, Seasonal riverine barium isotopic variation in the middle Yellow River: Sources and Fractionation, *Earth and Planetary Science Letters*, 531, doi:10.1016/j.epsl.2019.115990

Guay, C. K., and Falkner, K. K., 1997, Barium as a tracer of Arctic halocline and river waters, *Deep-Sea Research II,* 44 1543-1569

Guay C. K. and Falkner K. K., 1998, A survey of dissolved barium in the estuaries of major Arctic rivers and adjacent seas, *Continental Shelf Research*, 18, 859-882

Guay, C. K. H., Falkner, K. K., Muench, R. D., Mensch, M., Frank, M. and Bayer, R., 2001, Wind-driven transport pathways for Eurasian Arctic river discharge, *Journal of Geophysical Research,* 106, 11469-111480

Guay, C. K. H., McLaughlin, F. A. and Yamamoto-Kawai, M., 2009, Differentiating fluvial components of upper Canada Basin waters on the basis of measurements of dissolved barium combined with other physical and chemical tracers, *Journal of Geophysical Research*, 114, doi:10.1029/2008JC005099

Hanor J. S. and Chan L-H., 1977, Non-conservative behavior of barium during mixing of Mississippi River and Gulf of Mexico waters, *Earth and Planetary Science Letters***,** 37, 242-250

Haine, T. W. N., Curry, B., Gerdes, R., Hansen, E., Karcher, M., Lee, C., Rudels, B., Spreen, G., de Steur, L., Stewart, K. D. and Woodgate, R., 2015, Arctic freshwater export: Status, mechanisms, and prospects, *Global and Planetary Change*, 125, 13-35, doi:10.1016/j.gloplacha.2014.11.013

Hemsing F., Hsieh Y-T., Bridgestock L., Spooner P. T., Robinson L., F., Frank N. and Henderson G. M., 2018, Barium isotopes in cold-water corals, *Earth and Planetary Science Letters*, 491, 183-192, doi: 10.1016/j.epsl.2018.03.040

Hendry K. R., Pyle K. M., Butler G. B., Cooper A., Fransson A., Chierici M., Leng M. J., Meyer A. and Dodd P. A, 2018, Spatiotemporal variability of barium in Arctic sea-ice and seawater, *Journal of Geophysical Research: Oceans*, doi:10.1029/2017JC013668

Holmes, R.M., J.W. McClelland, S.E. Tank, R.G.M. Spencer, and A.I. Shiklomanov, 2021, Arctic Great Rivers Observatory, Water Quality Dataset, Version 20210319. https://www.arcticgreatrivers.org/data [Accessed, 26th April, 2021]

Horner T. J., Kinsley C. W. and Nielsen S. G., 2015, Barium-isotopic fractionation in seawater mediated by barite cycling and oceanic circulation, *Earth and Planetary Science Letters*, 430, 511-522, doi: 10.1016/j.epsl.2015.07.027

Horner T. J., Pryer H. V., Nielsen S. G., Crockford P. W., Gauglitz J. M., Wing B. A. and Ricketts R. D., 2017, Pelagic barite precipitation at micromolar ambient sulfate, *Nature Communications*, 8, 1242, doi:10.1038/s41467-017-01229-5

Hsieh Y-T. and Henderson G. M., 2017, Barium stable isotopes in the global ocean: Tracer of Ba inputs and utilization, *Earth and Planetary Science Letters*, 473, 269-278, doi: 10.1016/j.epsl.2017.06.024

Jacquet, S. H. M., Monnin, C., Riou, V., Jullion, L. and Tanhua, T., 2016, A high resolution and quasi-zonal transect of dissolved Ba in the Mediterranean Sea, *Marine Chemistry*, 178, 1-7, doi:10.1016/j.marchem.2015.12.001

Janout M. A., Aksenov Y., Hölemann J. A., Rabe B., Schauer U., Polyakov I. V., Bacon S., Coward A. C., Karcher M., Lenn Y-D., Kassens H. and Timokhov L., 2015, Kara Sea freshwater transport through Vilkitsky Strait: Variability, forcing, and further pathways toward the western Arctic Ocean from a model and observations, *Journal of Geophysical Research: Oceans*, doi:10.1002/2014JC010635

Johnson, M. A. and Polyakov, I. V., 2001, The Laptev Sea as a source for recent Arctic Ocean salinity changes, *Geophysical Research Letters*, 28, 2017-2020

Kipp L. E., Charette M. A., Moore W. S., Henderson P. B. and Rigor I. G., 2018, Increased fluxes of shelf-derived materials to the central Arctic Ocean, *Science Advances*, 4, doi:10.1126/sciadv.aao1302

Lambelet, M., Rehkamper, M., van de Flierdt, T., Xue, Z., Kreissig, K., Coles, B., Porcelli, D. and Andersson, P., 2013, Isotopic analysis of Cd in the mixing zone of Siberian rivers with the Arctic Ocean-New constraints on marine Cd cycling and the isotope composition of riverine Cd, *Earth and Planetary Science Letters*, 361, 64-73, doi:10.1016/j.epsl.2012.11.034

Macdonald, R. W., Carmack, E. C., McLaughlin, F. A., Falkner, K. K. and Swift, J. H., 1999, Connections among ice, runoff and atmospheric forcing in the Beaufort Gyre, *Geophysical Research Letters*, 26, 2223-2226

Mayfield, K. K., Eisenhauer, A., Santiago Ramos, D. P., Higgins, J. A., Horner, T. J., Auro, M., Magna, T., Moosdorf, N., Charette M. A., Gonneea, M. E., Brady, C. E., Komar, N., Peucker-Ehrenbrink, B. and Paytan, A., 2021, Groundwater discharge impacts marine isotope budgets of Li, Mg, Ca, Sr, and Ba, *Nature Communications*, doi:10.1038/s41467-020-20248-3

Meade R. H., Bobrovitskaya N. N. and Babkin V. I., 2000, Suspended-sediment and fresh-water discharges in the Ob and Yenisey rivers, 1960-1988, *In. J. Earth Sciences*, 89, 461-469, doi:10.1007/s005310000107

Milliman J. D., and Farnsworth K. L., 2011, River discharge to the coastal ocean: a global synthesis, Cambridge University Press

Morison, J., Kwok, R., Peralta-Ferriz, C., Alkire, M., Rigor, I., Andersen, R. and Steele, M., 2012, Changing Arctic Ocean freshwater pathways, *Nature,* 481, doi:10.1038/nature10705

Nan X-Y, Yu H-M., Rudnick R. L., Gaschnig R. M., Xu J., Li W-Y., Zhang Q., Jin Z-D, Li X-H. and Huang F., 2018, Barium isotopic composition of the upper continental crust, *Geochim. Cosmochim. Acta*, 233, 33-49, doi:10.1016/j.gca.2018.05.004

Nesbitt H. W., Markovics G. and Price R. C., 1980, Chemical processes affecting alkalis and alkaline earths during continental weathering, *Geochimica and Cosmochimica Acta*, 44, 1659-1666

Nozaki Y., Yamamoto Y., Manaka T., Amakawa H. and Snidvongs A., 2001, Dissolved barium and radium isotopes in the Chao Phraya River estuarine mixing zone in Thailand, *Continental Shelf Research,* 21, 1435-1448

Osadchiev A. A., Pisareva M. N., Spivak E. A., Shchuka S. A. and Semiletov I. P. , 2020, Freshwater transport between the Kara, Laptev, and East Siberian seas, *Scientific Reports*, 10:13041, doie:10.1038/s41598-020-70096-w

Proshutinski, A. Y., and Johnson, M. A., 1997, Two circulation regimes of the wind-driven Arctic Ocean, *Journal of Geophysical Research*, 102, 12,493-12,514

Proshutinsk, A., Dukhovskoy, D., Timmermans, M-L., Krishfield, R. and Bamber, J. L., 2015, Arctic circulation regimes, *Philosophical Transactions A*, 373, doi:10.1098/rsta.2014.0160

Rabe, B., Karcher, M., Kauker, F., Schauser, U., Toole, J. M., Krishfield, R. A., Pisarev, S., Kikuchi, T. and Su, J., 2014, Arctic Ocean basin liquid freshwater storage trend 1992-2012, *Geophysical Research Letters*, doi:10.1002/2013GL058121

Roeske, T., Bauch, D., Rutgers V.D Loeff, M. and Rabe, B., 2012, Utility of dissolved barium in distinguishing North American from Eurasian runoff in the Arctic Ocean, *Marine Chemistry,* 132-133, doi:10.1016/j.marchem.2012.01/007

Rosén, P-O., Andersson, P. S., Alling, V., Mörth, C-M., Björk, G., Semiletov, I., and Porcelli, D., 2015, Ice export from the Laptev and East Siberian Sea derived from $\delta^{18}O$, *Journal of Geophysical Research: Oceans*, 5997-6007, doi:10.1002/2015JC010866

Schlosser, P., Bauch, D., Fairbanks, R. and Bönisch, G., 1994, Arctic river-runoff: mean residence time on the shelves and in the halocline, *Deep-Sea Research I*, 41, 1053-1068

Shiller, A. M., Horner, T. J., 2021, Dissolved Ba, Cd, Cu, Ga, Mn, Ni, and V concentrations and Ba isotope concentrations from the US GEOTRACES Arctic Expedition (GN01, HLY1502) from August to October 2015. Biological and Chemical Oceanography Data Management Office (BCO-DMO). (Version 3) Version Date 2021-07-01 doi:10.26008/1912/bco-dmo.772645.3 [Accessed, 8th August, 2021]

Stecher H. A., and Kogut M. B., 1999, Rapid barium removal in the Delaware estuary, *Geochimica and Cosmochimica Acta*, 63, 1003-1012

Steele, M. and Boyd, T., 1998, Retreat of the cold halocline layer in the Arctic Ocean, *Journal of Geophysical Research,* 103, 10419-10435

Steele, M. and Ermold, W., 2004, Salinity trends on the Siberian shelves, *Geophysical Research Letters*, 31, doi:10.1029/2004GL021302

Taylor, J. R., Falkner, K. K., Schauer, U. and Meredith, M., 2003, Quantitative considerations of dissolved barium as a tracer in the Arctic Ocean, *Journal of Geophysical Research,* 108 doi:10.1029/2002JC001635

Thibodeau, B., Bauch, D., Kassens, H. and Timokhov, L. A., 2014, Interannual variations in river water content and distribution over the Laptev Sea between 2007 and 2011: The Arctic Dipole connections, *Geophysical Research Letters,* doi:10.1002/2014GL061814

Thomas H., Shadwick E., Dehairs F., Lansard B., Mucci A., Navez J., Gratton Y., Prowe F., Chierici M., Fransson A., Papakyriakou T. N., Sternberg E., Miller L. A., Tremblay J-E. and Monnin C., 2011, Barium and carbon fluxes in the Canadian Arctic Archipelago, *Journal of Geophysical Research,* 116, doi:10.1029/2011JC007120

Tian, L-L., Zeng, Z., Nan, X-Y., Yu, H-M. and Huang, F., 2019, Determining Ba isotopes of barite using the Na_2CO_3 exchange reaction and double-spike method by MC-ICP-MS, *J. Anal. At. Spectrom*, 34, 1459, doi:10.1039/c9ja00064j

Tieman, Z. G., Stewart, B. W., Capo, R. C., Phan, T., Lopano, C. and Hakala, J. A., 2020, Barium isotopes track the source of dissolved solids in produced water from the unconventional Marcellus shale gas play, *Environmental Science and Technology,* 54**,** 4275-4285, doi:10.1021/acs.est.0c00102

Wegner C., Bauch D., Hölemann J. A., Janout M. A., Heim B., Novikhin A., Kassens H. and Timokhov L., 2013, Interannual variability of surface and bottom sediment transport on the Laptev Sea shelf during summer, *Biogeosciences*, 10, 1117-1129, doi:10.5194/bg-10-1117-2013

Weingartner, T. J., Danielson, S., Sasaki, Y., Pavlov, V. and Kulakov, M., 1999, The Siberian Coastal Current: A wind- and buoyancy-forced Arctic coastal current, *Journal of Geophysical Research*, 104, 29697-29713

Whitmore, L. M., Shiller, A. M., Horner, T. J., Xiang, Y., Auro, M. E., Bauch, D., Dehairs, F., Lam, P. J., Li, J., Maldonado, M. T., Mears, C., Newton, R., Pasqualini, A., Planquette, H., Rember, R. and Thomas H., in revision, Strong margin influence on the Arctic Ocean barium cycle revealed by Pan-Arctic synthesis, *Journal of Geophysical Research: Oceans*, doi:10.1002/essoar.10506680.1

Williams, W. J. and Carmack, E. C., 2015, The 'interior' shelves of the Arctic Ocean: Physical oceanographic setting, climatology and effects of sea-ice retreat on cross-

shelf exchange, *Progress in Oceanography*, 139, 24-41, doi:10.1016/J.pocean.2015.07.008

Yamamoto-Kawai, M., McLaughlin, F. A., Carmack, E. C., Nishino, S. and Shimada, K., 2008, Freshwater budget of the Canada Basin, Arctic Ocean, from salinity, $\delta^{18}O$ and nutrients, *Journal of Geophysical Research*, 113, doi:10.1029/2006JC003858

Yamamoto-Kawai, M., Carmack, E. C., McLaughlin, F. A., and Falkner, K. K., 2010, Oxygen isotope ratio, barium and salinity in waters around the North American coast from the Pacific to the Atlantic: Implications for freshwater sources to the Arctic through flow, *Journal of Marine Research,* 68, 97-117,

Table 1, Barium concentration and $\delta^{138/134}$Ba results for Siberian shelf, Bering Sea/Strait and Lena River waters.

Station/ Group[a]	Latitude (°N)	Longitude (°E)	Depth (m)	Salinity	Ba concentration (nmol kg^{-1})		$\delta^{138/134}$Ba[c]
					ICP MS[b]	TIMS ID[b]	
International Siberian Shelf Study (August to September, 2008) on board the H/V Yacob Smirnitskyi							
YS2/Ob	73.405	72.9952	4	7.9	97.2	93.2	0.26
YS3/Yen	73.492	79.8848	4	7.3	49.6	49.9	0.35
YS4/L.N.	75.987	129.9842	3	11.4	75.8	77.6	0.29
YS6/L.N.	74.724	130.0163	3	5.2	90.8	92.8	0.30
YS11/L.E.	73.0185	129.9892	2.5	2.7	208.6	208.7	0.23
YS12/L.E.	71.9165	132.5757	4	24.9	94.1	92.9	0.29
YS13/ L.N.	71.968	131.7013	4	3.8	86.2	84.2	0.25
YS14/ L.N.	71.6303	130.0495	5	1.3	100.7	102.0	0.27
YS23/L.E.	72.789	142.6697	3	12.4	130.1	127.9	0.23
YS26/L.E.	72.4598	150.5957	8	24.3	100.0		
YS28/L.E.	72.6508	154.1853	4	19.7	83.4	61.7	0.28
YS30/L.E.	71.3577	152.1527	3	18.3	110.1	109.0	0.23
YS31/L.E.	71.1082	161.6935	3	23.2	78.3		
YS32/Koly.	70.5665	161.217	3.5	25.1	107.6		
YS34/Koly.	69.7082	162.6887	3	25.8	103.7		
YS35/Koly.	69.817	164.0568	3	29.5	81.2		
YS37/L.E.	70.1348	168.0068	3	27.6	38.2		
YS39/L.E.	71.2167	169.3472	2	27.5	59.4		
YS56/L.E.	71.8797	-175.3608	4	30.7	70.2	66.7	0.42
YS65/L.E.	72.3123	-176.137	4	29.3	58.8		
YS79/L.E.	73.704	-174.3297	4	26.0	62.6	60.6	0.38
YS81/L.E.	75.7995	179.9058	4	28.6	64.2		
YS90/L.E.	74.6682	172.3882	4	29.7	56.1	55.6	0.43
YS95/L.E.	74.4167	161.3353	4	23.9	73.6	72.3	0.31
YS101/L.E.	76.117	160.4572	4	25.8	68.8	66.9	0.38
YS108/L.E.	75.561	155.8827	4	25.0	75.3		
YS120/L.E.	73.2918	155.1675	4	20.9	99.0		
YS121/L.E.	74.3718	145.2808	4	17.6	108.0		
YS122/L.E.	74.5032	136.0097	1	15.7	104.9	102.1	0.26
YS126/L.N.	76.3657	132.618	4	19.7	55.4	55.5	0.45
YS128/L.N.	76.987	130.3557	4	20.7	59.9	61.2	0.42
GEOTRACES GN01 section cruise (August to October, 2015), on board the USCGC Healy							
Stn 1/B.Sea	60.252	-179.0655	4	32.9		40.9	0.55
Stn 3/B.Str	64.0069	-166.6259	4.5	31.8		37.6	0.55
Stn 5/BStr	66.3318	-168.9001	5.1	32.2		54.2	0.55
Lena River water (June, 2013)							
LR2013 45	68.89972222	124.2038889		0.0		85.5	0.27

[a]Sample grouping based on its location and influence of different water masses. Ob and Yen. denote samples influenced by the freshwater plumes of the rivers Ob and Yenisey, respectively. L.N. and L.E. denote samples influenced by the northward and eastward Lena freshwater plumes respectively. Koly. denotes samples influenced by freshwater input from the Kolyma River. B. Sea and B. Str. denote samples collected in the Bering Sea and Bering Strait respectively. [b]Barium concentrations measured by inductively coupled plasma mass spectrometry (ICP MS) and isotope dilution using thermal ionization mass spectrometry (TIMS ID). [c]Uncertainty of $\delta^{138/134}$ Ba assigned as ± 0.03 ‰ (2SD) based on long term reproduciblity of measurements of the standard reference material NIST3104a.

Table 2, Barium concentrations and $\delta^{138/134}$Ba of effective riverine and predicted Atlantic and Pacific derived endmembers derived from mixing relationships observed in Siberian Shelf surface water data

		Eastward Lena River plume	Northward Lena River plume
Effective River	**[Ba] nmol kg^{-1}**	197 ± 27	100 ± 11
	$\delta^{138/134}$Ba ‰	0.20 ± 0.06	0.25 ± 0.05
Predicted Atlantic	**[Ba] nmol kg^{-1}**	25 ± 15	28 ± 22
	$\delta^{138/134}$Ba ‰	0.73 ± 0.21	0.88 ± 0.28
Predicted Pacific	**[Ba] nmol kg^{-1}**	36 ± 14	33 ± 20
	$\delta^{138/134}$Ba ‰	0.55 ± 0.12	0.75 ± 22

Uncertainties are given by the 95% confidence intervals of the linear regressions used to define the mixing relationships (Fig. 3 and 4)

Table 3, Estimated Ba concentration and $\delta^{138/134}$Ba of major upper Arctic Ocean water sources

	Salinity	Ba concentration (nmol kg^{-1})	$\delta^{138/134}$Ba (‰)
Atlantic	34.92	43 ± 3	0.53 ± 0.06
Pacific	32.7	55 ± 5	0.55 ± 0.03
Eurasian river input	0	116 ± 9	0.23 ± 0.04
North American river input	0	520	Not available

Salinities and Ba concentrations of Atlantic and Pacific derived seawater and North American riverine inputs taken from Guay et al. (2009) and Roeske et al. (2012). The Ba concentration and $\delta^{138/134}$Ba of Eurasian river inputs are defined by the flux-weighted average of effective river endmember values for the rivers Yenisey, Lena and Ob presented in this study (section 5.2). The $\delta^{138/134}$Ba of Atlantic derived seawater is defined by literature data for North Atlantic surface waters (Bates et al., 2017, Hsieh and Henderson, 2017, Bridgestock et al., 2021; Supplementary Table 3), while that of Pacific derived seawater is defined by measurement of a surface water sample from the Bering Strait (this study).

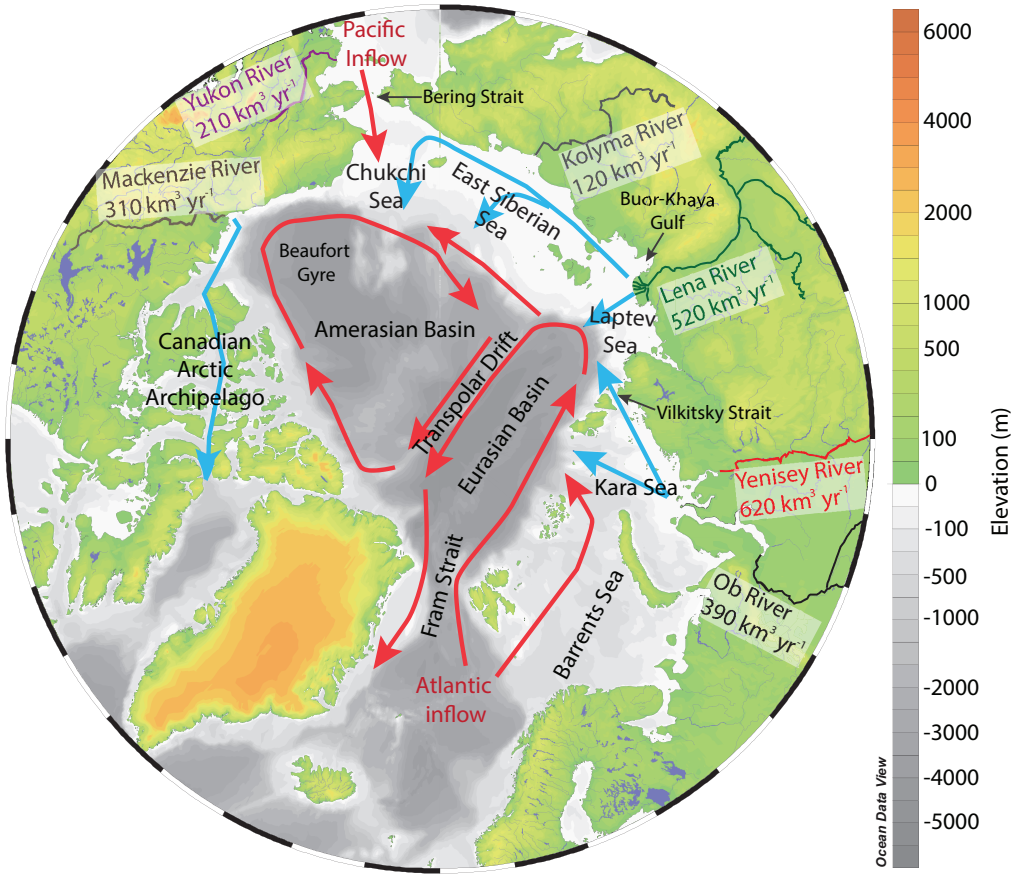

Figure 1, Major riverine freshwater and seawater sources to the Arctic Ocean with simplified surface circulation pattern. Blue arrows show transport pathways of major riverine freshwater inputs. The locations and discharges (Milliman and Farnsworth, 2011) of the 6 largest rivers for supplying freshwater to the Arctic Ocean are also shown.

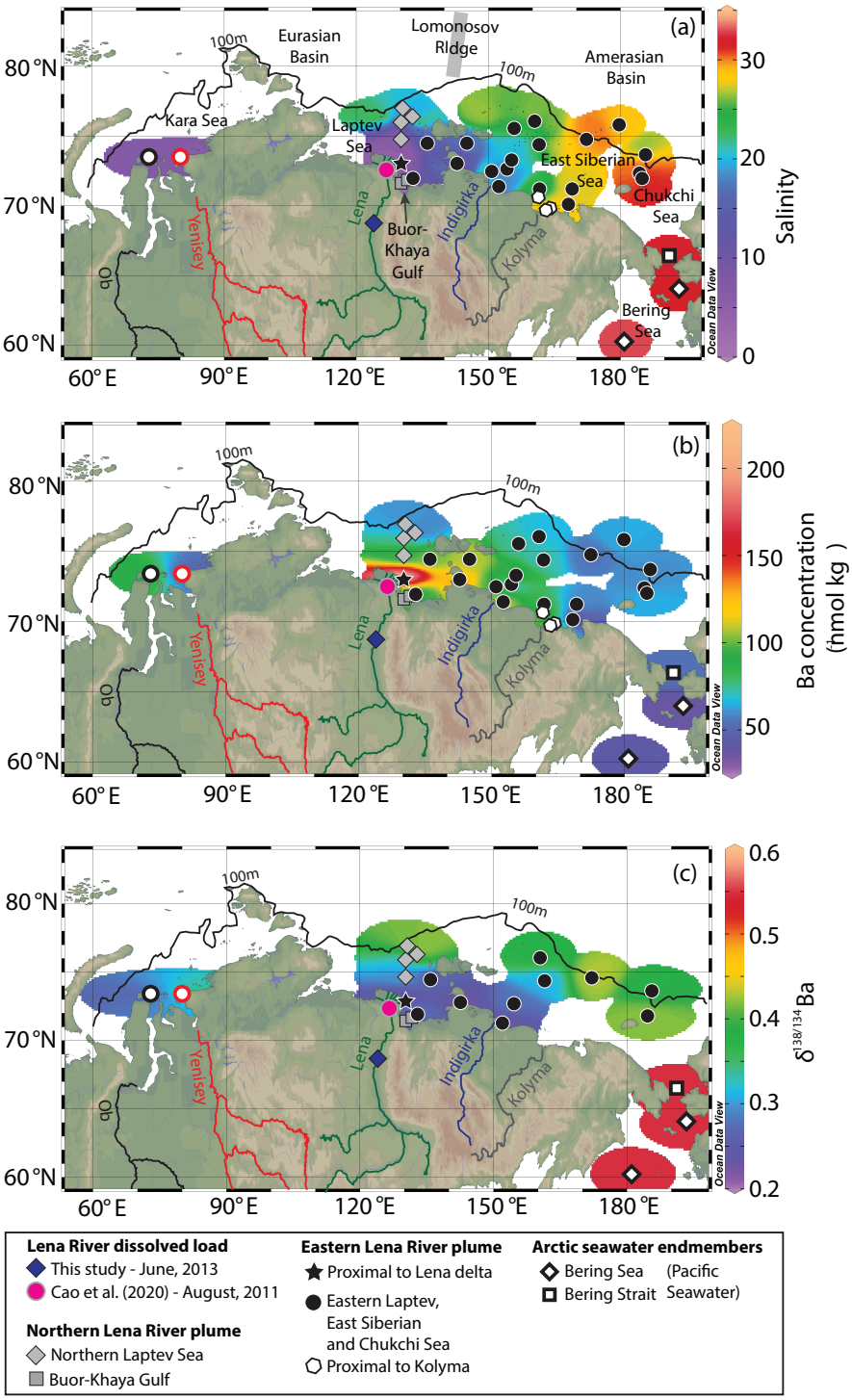

Figure 2, Sample locations and distributions of salinity (a), Ba concentration (b) and $\delta^{138/134}$Ba (c). The 100 m bathymetry contour is shown (solid black line) to denote the approximate position of the shelf break.

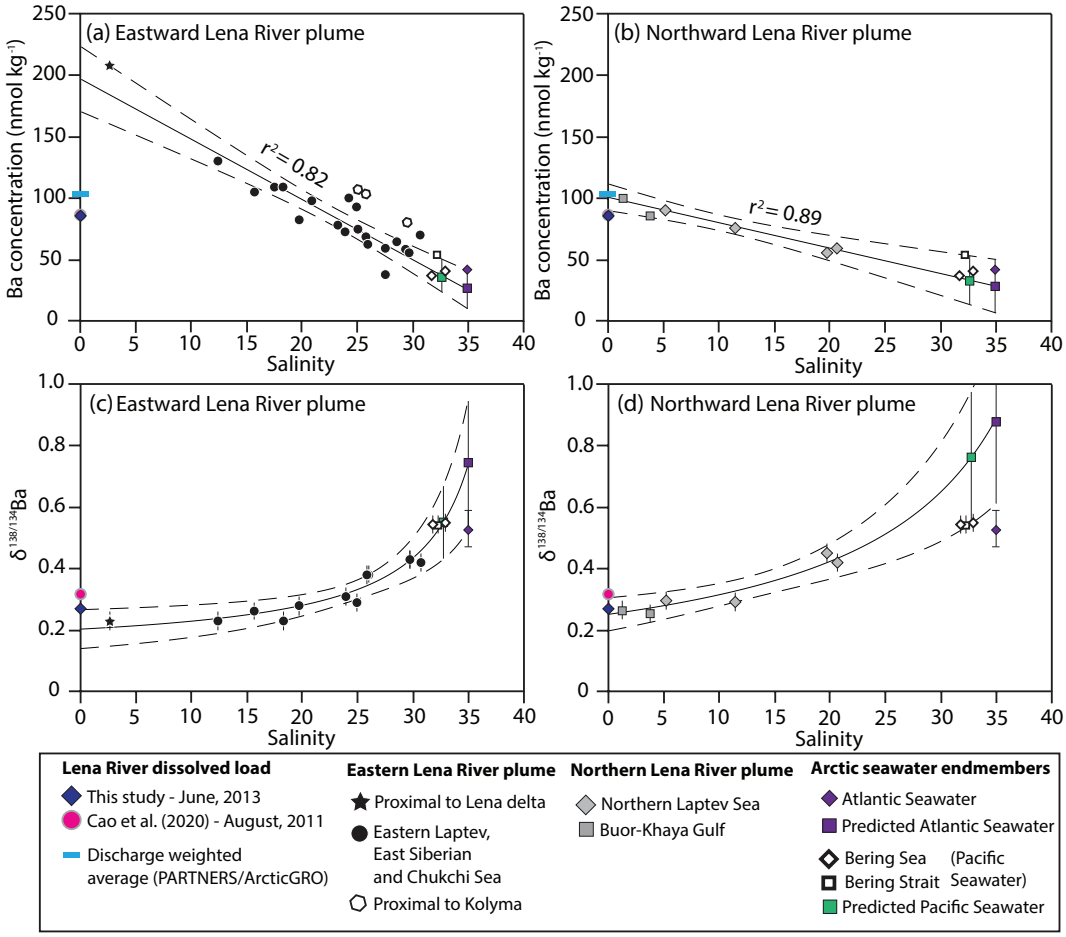

Figure 3, Relationships between salinity, Ba concentration and $\delta^{138/134}$Ba for the eastward and northward Lena River plumes. Solid black lines represent mixing relationships defined by linear regressions between Ba concentration and salinity in panels (a) and (b). In panels (c) and (d), mixing relationships are defined by linear regressions between 1/Ba concentration and $\delta^{138/134}$Ba (Fig. 4), which are combined with relationships between Ba concentration and salinity (panels (a) and (b)) to display as $\delta^{138/134}$Ba versus salinity. Dashed lines denote 95% confidence intervals. The discharge weighted average Ba concentration for the Lena River dissolved load (light blue bar, panels (a) and (b)) is based on time-series data spanning 2003 to 2016 (Cooper et al., 2008, Holmes et al. 2021).

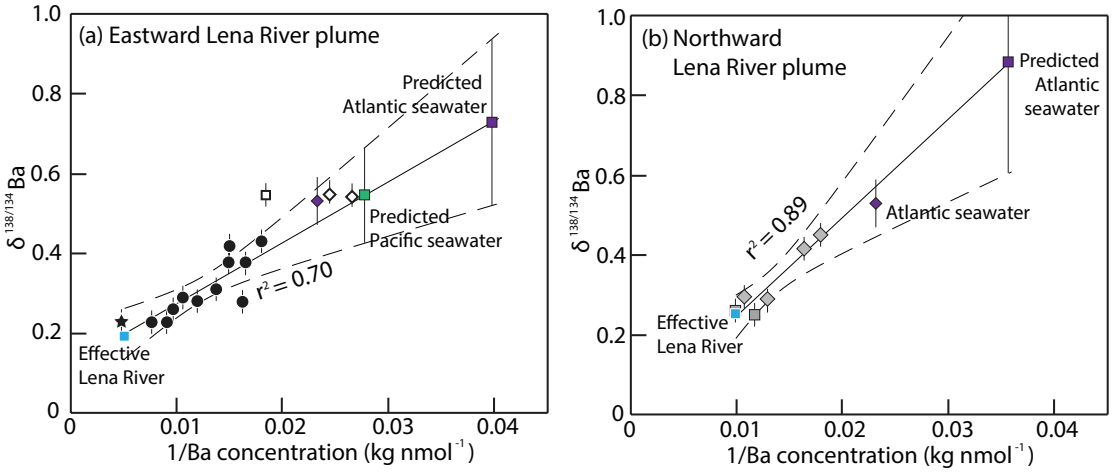

Figure 4, Relationships between $\delta^{138/134}$Ba and 1/Ba concentration for the eastward (panel a) and northward (panel b) Lena River freshwater plumes. Regressions are fit through the solid black (panel a) and grey (panel b) symbols, with dashed lines denoting 95% confidence intervals. Blue squares denote the effective Lena River endmembers defined by extrapolation of these relationships to salinity 0 (Fig. 3). The green (panel a) and purple (panel b) squares denote the predicted composition of Pacific and Atlantic derived water based on extrapolation of the mixing relationships to the salinities of these water sources (Fig. 3). The open squares and diamonds (panel a) denote data for samples collected in the Bering Sea and Strait, representing inflow of Pacific derived water. The purple diamond (panel b) denotes the composition of Atlantic derived seawater, based on compilation of available North Atlantic surface water (<100 m) literature data (Bates et al., 2017, Hsieh and Henderson, 2017, Bridgestock et al., submitted; Supplementary Table 3).

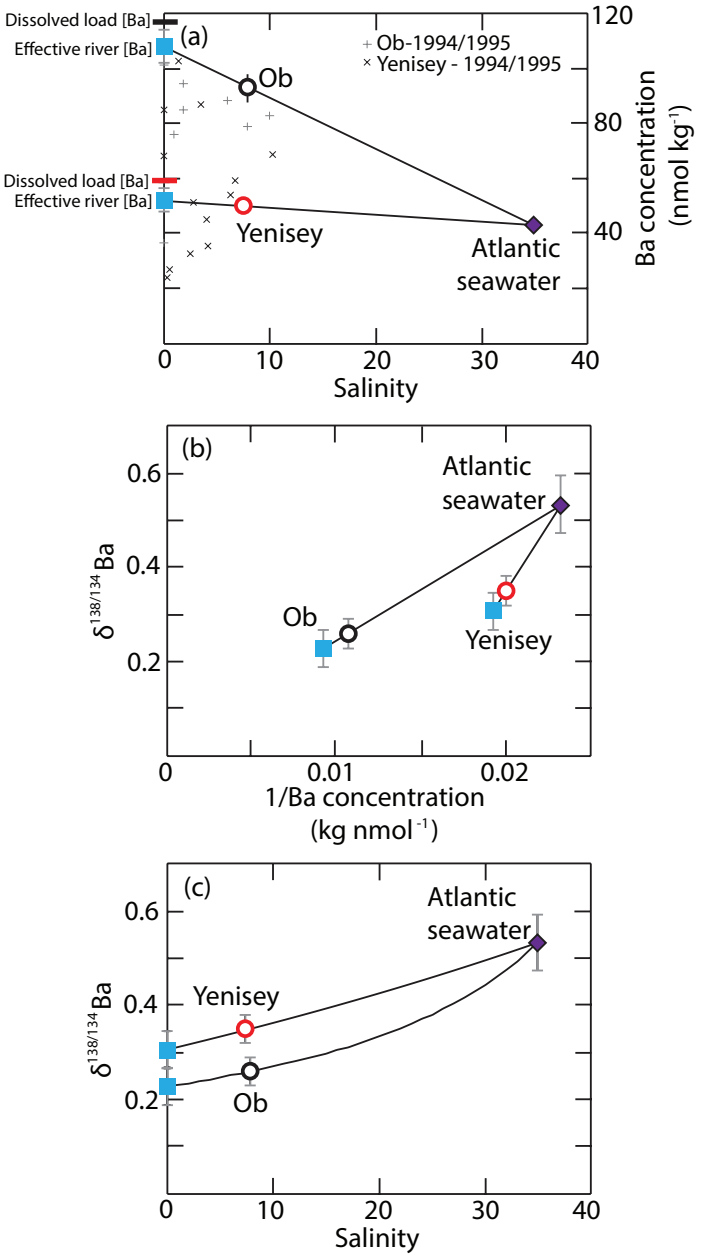

Figure 5, Inferred mixing relationships between freshwater discharged by the rivers Yenisey and Ob and Atlantic derived water (Bates et al., 2017, Hsieh and Henderson, 2017, Bridgestock et al., submitted; Supplementary Table 3). Blue rectangles show estimated effective river endmembers for the Yenisey and Ob rivers. The red and black bars in panel (a) show the discharge weighted average Ba concentrations of the dissolved loads of the rivers Yenisey and Ob respectively, based on time-series data spanning 2003 to 2016 (Cooper et al., 2008, Holmes et al. 2021). The grey and black

crosses in panel (a) show literature data for the river Ob and Yenisey freshwater plumes sampled in 1994 and 1995 (Guay and Falkner, 1998).

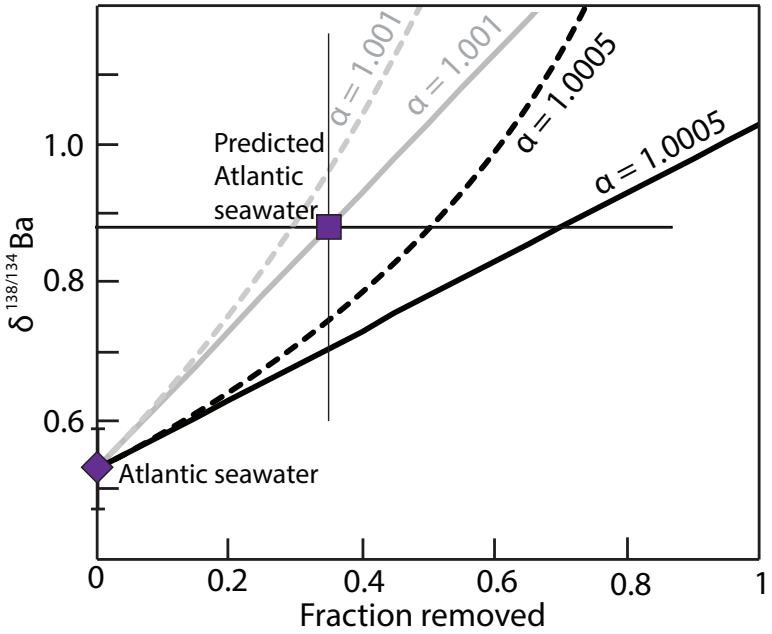

Figure 6, Inferred impact of non-conservative processes on the $\delta^{138/134}$Ba of Atlantic-derived seawater along the Laptev Sea shelf break. Fraction removed denotes the amount of Ba removed by non-conservative processes relative to the Ba concentration of Atlantic-derived water. Solid and dashed lines show batch (eqn. 2) and Rayleigh (eqn. 3) fractionation models respectively.

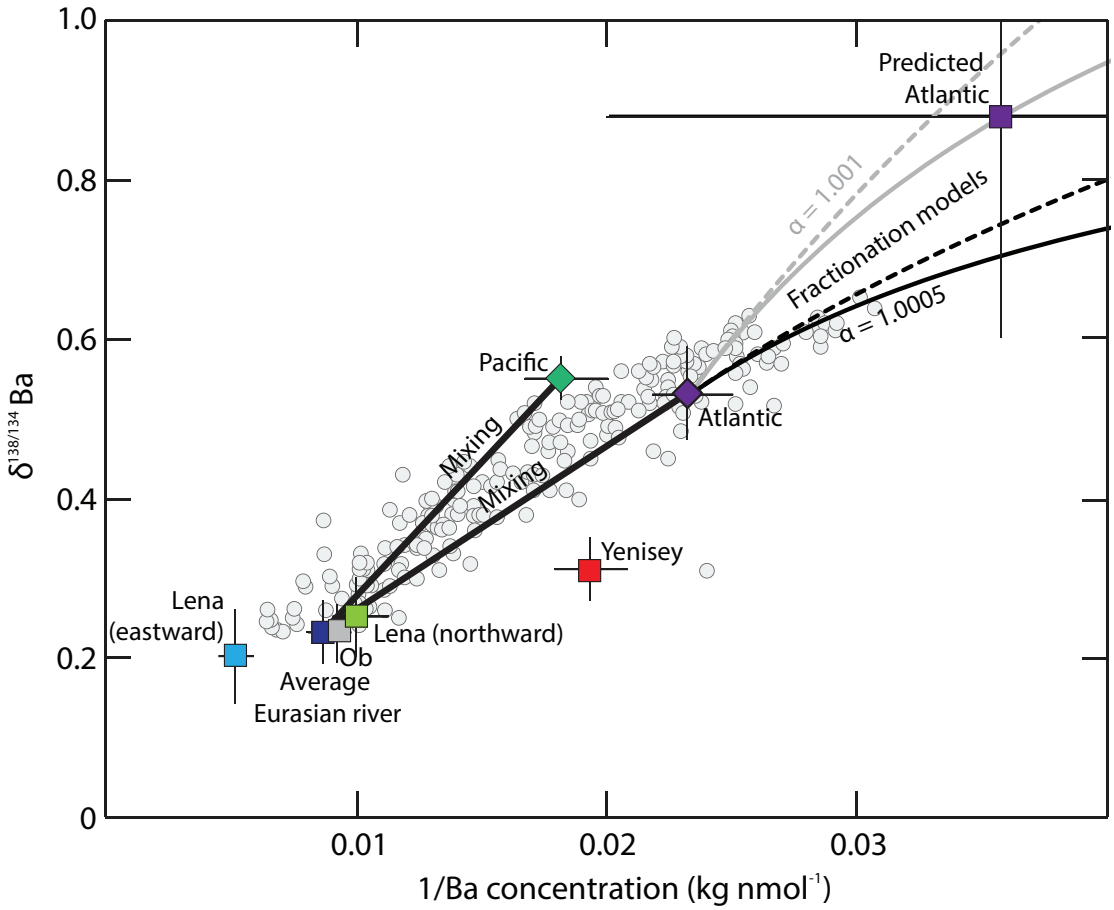

Figure 7, Comparison of dissolved Ba concentration-$\delta^{138/134}$Ba relationships resulting from mixing between Arctic Ocean seawater and Eurasian river water, and non-conservative processes. Thick black lines show mixing relationships between Atlantic/Pacific-derived Arctic Ocean seawater and average Eurasian River freshwater, which are linear in this plot. Thin black and grey lines show batch (solid) and Rayleigh (dashed) fractionation models. Grey circles show literature seawater data, which globally lie on a single relationship generated by isotope fractionation during non-conservative cycling of Ba between the upper and deep ocean and water mass mixing (Horner et al., 2015, Bates et al., 2017, Hsieh and Henderson, 2017, Bridgestock et al., 2018, Hemsing et al., 2018, Geyman et al., 2019, Cao et al., 2020a).

Supplementary Information for

Assessing the utility of barium isotopes to trace Eurasian riverine freshwater inputs to the Arctic Ocean

Luke Bridgestock[1]*, Joseph Nathan[1], Yu-Te Hsieh[1], Phil Holdship[1], Don Porcelli[1], Per S. Andersson[2] and Gideon M. Henderson[1]

[1]Department of Earth Science, University of Oxford, South Parks Road, Oxford, OX1 3AN, UK

[2]Laboratory for Isotope Geology, Swedish Museum of Natural History, Stockholm Sweden

*Corresponding author; ljb212@cam.ac.uk

Present address (Luke Bridgestock): Department of Earth Sciences, University of Cambridge, Downing Street, Cambridge, CB2 3EQ, UK

1. Ion exchange chromatography procedure for the purification of Ba from sample matrices prior to isotopic analysis

The $CaCO_3$ precipitates were dissolved in 3M HCl and processed twice through the cation exchange chromatography procedure described in Supplementary Table 1. The dried residue of the Lena River water sample was dissolved in 3M HCl and processed once through this cation exchange chromatography procedure. This procedure utilized AG50-X8 resin (200-400 mesh) and Teflon shrink fit columns with a resin bed volume of 2 ml and aspect ratio (diameter: length) of 0.05.

Supplementary Table 1, Cation exchange chromatography procedure used to purify Ba from sample matrix prior to isotopic analyses

Step	**Regent**
Clean resin	20 ml H_2O
	20 ml 6M HCl
Condition resin	20 ml 3M HCl
Load sample	1 ml 3M HCl
Elute matrix	18 ml 3M HCl
Elute Ba	10 ml 4M HNO_3

Supplementary Table 2, Barium concentration results for in house seawater standards and certified reference material measured using PerkinElmer NexION 350D quadrupole ICP-MS

	Ba concentration (nmol kg^{-1})	2SD	n	Literature/consensus value (nmol kg^{-1})
South Atlantic seawater[a]	51.9	± 1.8	11	51.4
North Atlantic seawater[b]	45.4	± 0.6	3	44.7
SLRS-6[c]	100.3	± 3.3	2	104.1 ± 3.5

[a]South Atlantic seawater sample collected during the GEOTRACES GA10 section cruise, station 18 (40.00 °S, -42.42 °E), 195 m water depth. Literature value represents the average of 2 replicate measurements of the water sample from 199 m, at the same station (Bridgestock et al., 2018).
[b]North Atlantic seawater sample collected at Hydrostation S (32.17 °N, -64.50 °E), 10m water depth, with published Ba concentration value from Hsieh & Henderson, 2017.
[c] River water certified reference material (National Research Council Canada)

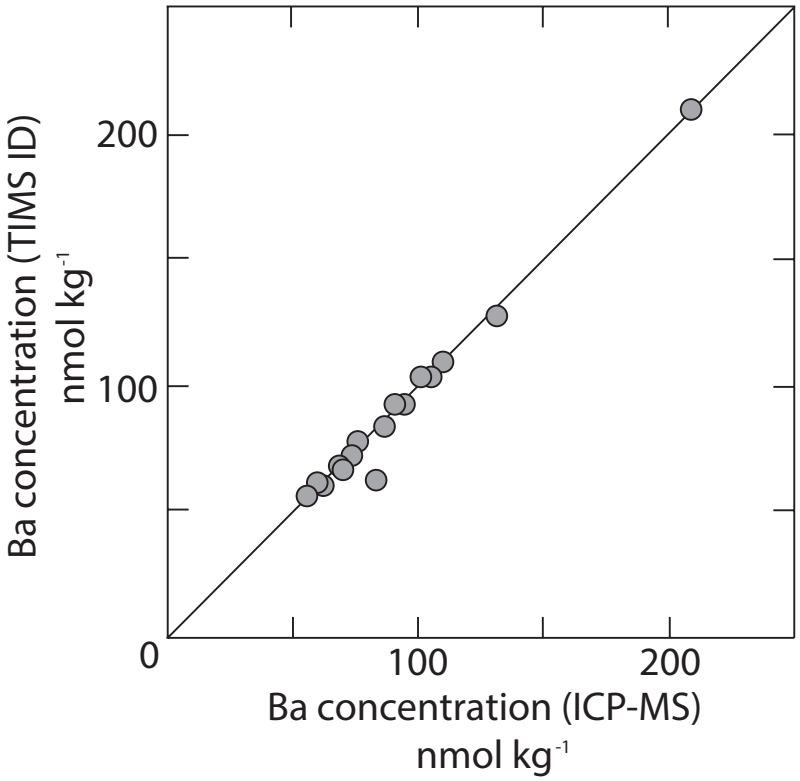

Supplementary Figure 1, Comparison of Ba concentrations determined using isotope dilution based on thermal ionization mass spectrometry analyses (TIMS ID) and inductively coupled plasma mass spectrometry (ICP-MS). Black line denotes 1:1 relationship. All results agree within 5% with the exception of a single sample from station YS28 for which the ICP-MS result is 26% higher than the TIMS ID.

2. Intercalibration of GEOTRACES GN01 section dissolved Ba concentration and $\delta^{138/134}$Ba data

Seawater samples collected during the GEOTRACES GN01 section cruise at stations 1, 3 and 5 have also been analyzed for dissolved Ba concentrations and isotope $\delta^{138/134}$Ba values by Shiller and Horner (2021) (Whitmore et al., in revision) (Supplementary Fig. 2). Data from Shiller and Horner/Whitmore et al. were produced from samples collected using the GEOTRACES Clean Carousel sampling system, while that from this study are for samples collected using the ODF stainless steel rosette, equipped with Niskin bottles. Surface samples from stations 1, 3 and 5 from these two different sample sets are from slightly different depths and locations, featuring differences in salinity, particularly at station 5 (Supplementary Table 3; Supplementary Figure 2). Dissolved Ba concentrations agree within 12% between the two datasets, while $\delta^{138/134}$Ba values agree within 0.05 to 0.13 ‰. This agreement between $\delta^{138/134}$Ba values is slightly outside of the analytical uncertainty of the data (± 0.03 to 0.05 ‰; 2SD). The largest disagreement between $\delta^{138/134}$Ba values of 0.13 ‰ is observed at station 5. Samples from these stations also feature a significant difference in salinity likely due to the slight difference in depth and location of the two sample sets. This variance in $\delta^{138/134}$Ba values could therefore at least partly reflect genuine differences in the sampled seawater rather than disagreement between analytical methods. Another possibility is that these differences could be caused by differences in the sampling systems used to collect the two sample sets. In particular, samples in this study were collected using the ODF stainless steel rosette, which is more prone to contamination risk than the GEOTRACES Clean Carousel sampling system. Such contamination during sampling would be characterized by systematically higher Ba concentrations in the data of this study compared to the

Shiller and Horner/Whitmore et al. dataset. This is, however, not consistent with observations (Supplementary Table 3; Supplementary Figure 2).

Supplementary Table 3, Comparison of dissolved Ba concentration and $\delta^{138/134}$Ba data for GEOTRACES section GN01 samples from this study and Shiller and Horner (2021)/Whitmore et al. (in revision)

Station	Latitude (°N)	Longitude (°E)	Depth (m)	Salinity	[Ba] nmol kg $^{-1}$	$\delta^{138/134}$Ba	2SD
This study							
1	60.2520	-179.0655	4	32.90	40.9	0.55	0.03
3	64.0069	-166.6259	4.5	31.76	37.6	0.55	0.03
5	66.3318	-168.9001	5.1	32.24	54.2	0.55	0.03
Shiller and Horner (2021) /Whitmore et al. (in revision)							
1	60.2579	-179.0832	24.3	32.93	38.7	0.50	0.04
3	64.0040	-166.6097	18.5	31.75	42.2	0.48	0.05
5	66.3284	-168.9007	16.7	32.59	59.3	0.42	0.04

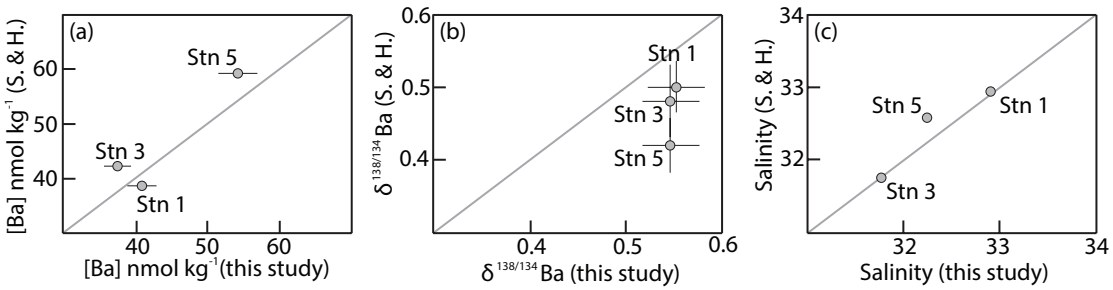

Supplementary Figure 2, Comparison of Ba concentration and $\delta^{138/134}$Ba values for surface waters from GEOTRACES GN01 section cruise at stations 1, 3 and 5 determined by this study and Shiller and Horner (2021)/Whitmore et al., (in revision) (S. & H)

3. Estimation of effective river Ba concentrations and $\delta^{138/134}$Ba values

Effective river endmember values, which are the theoretical Ba concentration or $\delta^{138/134}$Ba value of a parcel of river water after modification by estuarine processes, are estimated by extrapolation of mixing relationships observed at higher salinity regions of estuaries to salinity 0 (Fig. 3, Fig. 5; main article). Mixing relationships between Ba concentration and salinity are linear, so that the effective Ba concentration is obtained as the y-intercept of linear regressions between these variables. Mixing relationships between $\delta^{138/134}$Ba and salinity (and Ba concentration) are, however, non-linear, but $\delta^{138/134}$Ba versus 1/Ba concentration is linear. Extrapolation of linear regressions between $\delta^{138/134}$Ba versus 1/Ba concentration to the reciprocal of the effective river Ba concentration provides an estimate of the effective river $\delta^{138/134}$Ba value (Fig. 4, main article). Note that in figure 3, panels (c) and (d), the mixing relationships between $\delta^{138/134}$Ba and salinity are derived by combining linear regressions between $\delta^{138/134}$Ba versus 1/Ba concentration (Fig. 4, main article) with those for Ba concentration versus salinity (Fig. 3a, main article). Uncertainties on effective river Ba concentrations and $\delta^{138/134}$Ba values are given by the 95% confidence intervals of these linear regressions.

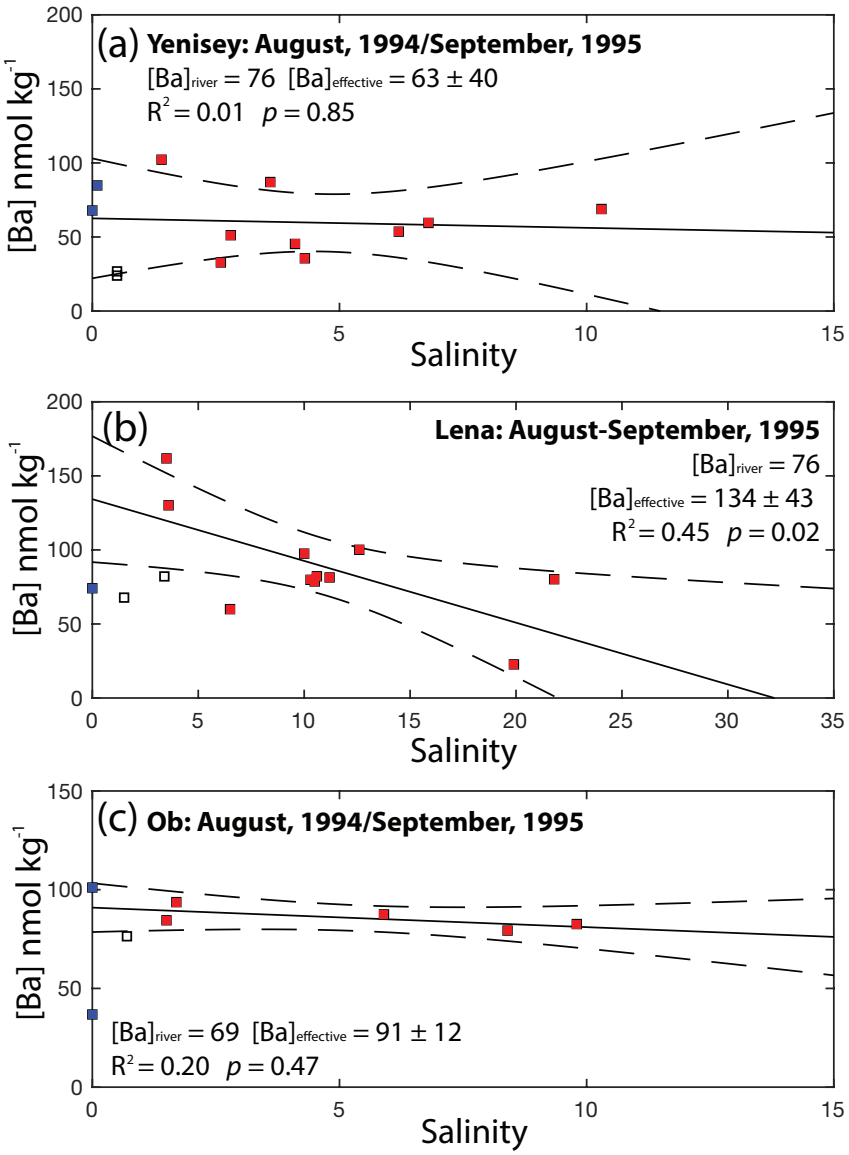

Supplementary Figure 3, Dissolved Ba concentration distributions across the estuarine mixing zones of the rivers Yenisey, Lena and Ob determined for samples collected in 1994/1995 (Guay and Falkner, 1998). Blue squares indicate data used to constrained the Ba concentration of the river dissolved loads ($[Ba]_{river}$). Red squares indicate the data used to constrain the Ba concentration of the effective river endmembers ($[Ba]_{effective}$) using linear regressions (solid black lines) with uncertainties given by the 95% confidence intervals (dashed black lines).

4. Constraints on the $\delta^{138/134}$Ba of Atlantic derived seawater in the Arctic Ocean

The $\delta^{138/134}$Ba of Atlantic-derived water in the Arctic Ocean is constrained by literature data for North Atlantic surface seawater (< 100 m) (Bates et al., 2017, Hsieh and Henderson, 2017, Bridgestock et al., 2021) (Supplementary Table 4). This currently available data unfortunately does not include samples collected at latitudes higher than 32.17 °N, which would be better suited to defining the $\delta^{138/134}$Ba of Atlantic-derived seawater in the Arctic Ocean. The Ba concentrations of these samples (41 ± 7 nmol kg^{-1}, 2SD), however, agree with that determined for Atlantic-derived Arctic seawater (43± 3 nmol kg^{-1}; Roeske et al., 2012, Guay et al., 2009) supporting the choice of this endmember $\delta^{138/134}$Ba value, given that dissolved Ba concentration and $\delta^{138/134}$Ba are tightly coupled in open ocean settings (e.g. Hsieh and Henderson, 2017).

Supplementary Table 4, Literature compilation of surface (<100 m depth) seawater $\delta^{138/134}$Ba data from the North Atlantic used to define the $\delta^{138/134}$Ba of Atlantic derived seawater in the Arctic Ocean

Latitude (°N)	**Longitude (°E)**	**Depth (m)**	**Salinity**	**Ba concentration (nmol kg^{-1})**	**$\delta^{138/134}$Ba**
32.17	-64.50	11	36.67	44.7	0.52 ± 0.02[a]
32.17	-64.50	51	36.61	44.3	0.53 ± 0.02[a]
32.17	-64.50	100	36.66	44.9	0.52 ± 0.02[a]
9.28	-21.63	11		37.9	0.57 ± 0.04[b]
9.28	-21.63	55		45.7	0.46 ± 0.04[b]
10.85	-44.49	12		38.9	0.54 ± 0.06[b]
10.85	-44.49	76		39.8	0.56 ± 0.03[b]
15.27	-48.27	16		42.1	0.52 ± 0.03[b]
15.27	-48.27	95		39.8	0.56 ± 0.03[b]
6.87	-52.94	Surface	35.84	37.4	0.54 ± 0.03[c]
Mean (±2SD)				**41 ± 7**	**0.53 ± 0.06**

[a]Hsieh and Henderson (2017) [b]Bates et al. (2017) [c]Bridgestock et al. (2021)

References

Bates S. L., Hendry K. R., Pryer H. V., Kinsley C. K., Pyle K. M., Woodward E. M. and Horner T. J. (2017) Barium isotopes reveal role of ocean circulation on barium cycling in the Atlantic*, Geochim.Cosmochim. Acta*, 204, 286-299, doi: 10.1016/j.gca.2017.01.043

Bridgestock, L., Hsieh, Y-T., Porcelli, D., Homoky, W. B., Bryan, A. and Henderson, G. M., 2018, Controls on the barium isotope compositions of marine sediments, *Earth and Planetary Science Letters*, 481, 101-110, doi: 10.1016/j.epsl.2017.10.019

Bridgestock, L., Nathan, J., Paver, R., Hsieh, Y-T. Porcelli, D., Tanzil, J., Holdship, P., Carrasco, G., Annammala, K. V., Swarzenski', P. W., and Henderson, G. M., 2021, Estuarine processes modify the isotope composition of dissolved riverine barium fluxes to the ocean, *Chemical Geology,* 579, doi:10.1016/j.chemgeo.2021.120340

Guay C. K. and Falkner K. K., 1998, A survey of dissolved barium in the estuaries of major Arctic rivers and adjacent seas, *Continental Shelf Research*, 18, 859-882

Guay, C. K. H., McLaughlin, F. A. and Yamamoto-Kawai, M., 2009, Differentiating fluvial components of upper Canada Basin waters on the basis of measurements of dissolved barium combined with other physical and chemical tracers, *Journal of Geophysical Research*, 114, doi:10.1029/2008JC005099

Hsieh, Y-T. and Henderson, G. M., 2017, Barium stable isotopes in the global ocean: Tracer of Ba inputs and utilization, *Earth and Planetary Science Letters*, 473, 269-278, doi: 10.1016/j.epsl.2017.06.024

Roeske, T., Bauch, D., Rutgers V.D Loeff, M. and Rabe, B., 2012, Utility of dissolved barium in distinguishing North American from Eurasian runoff in the Arctic Ocean, *Marine Chemistry,* 132-133, doi:10.1016/j.marchem.2012.01/007

Shiller, A. M., Horner, T. J. (2021) Dissolved Ba, Cd, Cu, Ga, Mn, Ni, and V concentrations and Ba isotope concentrations from the US GEOTRACES Arctic Expedition (GN01, HLY1502) from August to October 2015. Biological and Chemical Oceanography Data Management Office (BCO-DMO). (Version 3) Version Date 2021-07-01 doi:10.26008/1912/bco-dmo.772645.3 [Accessed, 8th August, 2021]

Whitmore, L. M., Shiller, A. M., Horner, T. J., Xiang, Y., Auro, M. E., Bauch, D., Dehairs, F., Lam, P. J., Li, J., Maldonado, M. T., Mears, C., Newton, R., Pasqualini, A., Planquette, H., Rember, R. and Thomas H., in revision, Strong margin influence on the Arctic Ocean barium cycle revealed by Pan-Arctic synthesis, *Journal of Geophysical Research: Oceans*, doi:10.1002/essoar.10506680.1